

AD _____

AWARD NUMBER DAMD17-97-1-7261

TITLE: Non-Invasive Determination of Breast Cancer Oxygen Tension by F-19 NMR and Breast Cancer Physiology in Response to Radiotherapy

PRINCIPAL INVESTIGATOR: Yulin Song

CONTRACTING ORGANIZATION: University of Texas
Southwestern Medical Center
Dallas, Texas 75235-9106

REPORT DATE: August 1999

TYPE OF REPORT: Annual

PREPARED FOR: Commander
U.S. Army Medical Research and Materiel Command
Fort Detrick, Maryland 21702-5012

DISTRIBUTION STATEMENT: Approved for public release; distribution unlimited

The views, opinions and/or findings contained in this report are those of the author(s) and should not be construed as an official Department of the Army position, policy or decision unless so designated by other documentation.

DTIC QUALITY INSPECTED 4

20001017 052

REPORT DOCUMENTATION PAGE

Form Approved
OMB No. 0704-0188

Public reporting burden for this collection of information is estimated to average 1 hour per response, including the time for reviewing instructions, searching existing data sources, gathering and maintaining the data needed, and completing and reviewing the collection of information. Send comments regarding this burden estimate or any other aspect of this collection of information, including suggestions for reducing this burden, to Washington Headquarters Services, Directorate for Information Operations and Reports, 1215 Jefferson Davis Highway, Suite 1204, Arlington, VA 22202-4302, and to the Office of Management and Budget, Paperwork Reduction Project (0704-0188), Washington, DC 20503.

1. AGENCY USE ONLY <i>(Leave blank)</i>	2. REPORT DATE August 1999	3. REPORT TYPE AND DATES COVERED Annual (1 Aug 98 - 31 Jul 99)	
4. TITLE AND SUBTITLE Non-Invasive Determination of Breast Cancer Oxygen Tension by F-19 NMR and Breast Cancer Physiology in Response to Radiotherapy		5. FUNDING NUMBERS DAMD17-97-1-7261	
6. AUTHOR(S) Yulin Song		8. PERFORMING ORGANIZATION REPORT NUMBER	
7. PERFORMING ORGANIZATION NAME(S) AND ADDRESS(ES) University of Texas Southwestern Medical Center Dallas, Texas 75235-9106			
9. SPONSORING / MONITORING AGENCY NAME(S) AND ADDRESS(ES) U.S. Army Medical Research and Materiel Command Fort Detrick, Maryland 21702-5012		10. SPONSORING / MONITORING AGENCY REPORT NUMBER	
11. SUPPLEMENTARY NOTES			
12a. DISTRIBUTION / AVAILABILITY STATEMENT Approved for public release; distribution unlimited		12b. DISTRIBUTION CODE	
13. ABSTRACT <i>(Maximum 200 words)</i> me The goals of this fellowship are to provide with the solid and extensive training and valuable experience in a modern NMR laboratory for a career as a clinical medical physicist and a breast cancer research scientist and to develop and investigate a non-invasive technique of measuring oxygen tension in breast cancer based on ¹⁹ F MRI of hexafluorobenzene (HFB). In terms of training, I have learned tumor biology, surgical techniques for implanting breast tumors, MRI data acquisitions, digital signal and image processing, and operation of advanced instruments. In terms of research, we found that HFB decays exponentially with a typical biological half-life ranging from 700 to 1200 min. We also found that tumor voxels with high baseline pO ₂ had different response characteristics from those with initially low pO ₂ and time constants of well-oxygenated voxels were much shorter than those of hypoxic voxels. A comparison between ¹⁹ F EPI and NIR showed that the global time constant of pO ₂ was much longer than that of blood hemoglobin saturation (sO ₂) and changes in tumor vascular sO ₂ preceded tumor tissue pO ₂ , particularly for small tumors. Our preliminary results indicated that pO ₂ and its distribution in tumors changed with tumor growth and there existed heterogeneity in pO ₂ distribution.			
14. SUBJECT TERMS Breast Cancer , Hexafluorobenzene (HFB), Perfluorocarbon (PFC), ¹⁹ F-NMR, Echo planar imaging (EPI), and NIR spectroscopy		15. NUMBER OF PAGES 39	
17. SECURITY CLASSIFICATION OF REPORT Unclassified		16. PRICE CODE	
		20. LIMITATION OF ABSTRACT Unlimited	
18. SECURITY CLASSIFICATION OF THIS PAGE Unclassified		19. SECURITY CLASSIFICATION OF ABSTRACT Unclassified	

FOREWORD

Opinions, interpretations, conclusions and recommendations are those of the author and are not necessarily endorsed by the U.S. Army.

____ Where copyrighted material is quoted, permission has been obtained to use such material.

____ Where material from documents designated for limited distribution is quoted, permission has been obtained to use the material.

____ Citations of commercial organizations and trade names in this report do not constitute an official Department of Army endorsement or approval of the products or services of these organizations.

In conducting research using animals, the investigator(s) adhered to the "Guide for the Care and Use of Laboratory Animals," prepared by the Committee on Care and use of Laboratory Animals of the Institute of Laboratory Resources, National Research Council (NIH Publication No. 86-23, Revised 1985).

____ For the protection of human subjects, the investigator(s) adhered to policies of applicable Federal Law 45 CFR 46.

____ In conducting research utilizing recombinant DNA technology, the investigator(s) adhered to current guidelines promulgated by the National Institutes of Health.

____ In the conduct of research utilizing recombinant DNA, the investigator(s) adhered to the NIH Guidelines for Research Involving Recombinant DNA Molecules.

In the conduct of research involving hazardous organisms, the investigator(s) adhered to the CDC-NIH Guide for Biosafety in Microbiological and Biomedical Laboratories.

Serg Yuliev 9-10-99
PI - Signature Date

TABLE OF CONTENTS

Front Cover	1
Report Documentation Page (Standard Form 298)	2
Foreword	3
Table of Contents	4
I. Introduction	5
II. Training Accomplishments	5
III. Research Accomplishments	6
IV. Appendices	10
1) A List of Key Research Accomplishments	10
2) A List of Reportable Outcomes	11
3) Copies of Manuscripts and Abstracts	12

I. INTRODUCTION

The fundamental goals of this predoctoral fellowship are three-fold: 1) to provide me with an opportunity to continue to learn and apply the state of the art NMR technology and radiotherapy techniques to cancer diagnosis and treatment; 2) to provide me with the solid and extensive training, and valuable experience in a modern NMR laboratory for a career as a clinical diagnostics and radiation therapy physicist and a breast cancer research scientist; and 3) to develop and investigate a non-invasive technique of measuring oxygen tension (pO_2) in breast cancers based on ^{19}F MRI of hexafluorobenzene (HFB), now called the FREDOM (Fluorocarbon Relaxometry using Echo planar imaging for Dynamic Oxygen Mapping). Under the guidance of my mentor, Dr. Ralph P. Mason, I have gone through a rigorous training in tumor biology, surgical techniques for implanting breast tumors, MRI data acquisitions, digital signal and image processing, and using other advanced instruments. In the meantime, I have also done many experiments using both the FREDOM and the near infrared (NIR) spectroscopy techniques to investigate breast tumor oxygenation accompanying respiratory challenges. In addition, I have been developing a new pO_2 mapping software using MS Visual Basic 6.0 and building new MRI/NIR coils. Some of the research results and findings have been presented at various international conferences. In this report, I will briefly describe some of the highlights of my past year's training and research. For further information regarding the research results, please refer to the Appendices.

II. TRAINING ACCOMPLISHMENTS

This project primarily uses an Omega CSI 4.7 T MR system with actively shielded gradients (AcustarTM, Bruker Instruments, Inc., Fremont, CA, USA). This system, based on a 40-cm diameter bore horizontal magnet, is located in the Rogers Magnetic Resonance Center and is an NIH Biotechnology Resource Facility. I have immediate access to the system and, on average, used three days per week in the past for either experiments or programming. Now I can operate the system independently for both imaging and spectroscopy. To meet our particular needs, I also modified and wrote some NMR-shell based data acquisition and post-processing programs. At present, I am learning and developing a new program based on our current ^{19}F PBSR-EPI program. This new program will enable us to acquire pO_2 data based on BOLD (blood oxygen level dependent) effect. The BOLD techniques are completely non-invasive and provide qualitative indications of tumor oxygenation on the basis of magnetic susceptibility gradient changes around vasculature. This will allow us to compare the BOLD results with those obtained using the FREDOM and NIR spectroscopy. This project also involves the investigation of tumor physiology, which requires the use of rat tumors and implanting mammary adenocarcinoma 13762 NF in female Fisher rats is a complicated surgical procedure. Now I have learned the techniques and can do the surgery with confidence. In addition, I have also learned the techniques of blood gas analysis using fiber optic pulse oximeter and how to use automated microelectrode systems. As an important part of my Ph.D. training and research, I have been developing a new pO_2 mapping software using MS Visual Basic 6.0. This is a windows-based software that allows us to perform many special operations on the data.

III. RESEARCH ACCOMPLISHMENTS

It is widely appreciated that tumor oxygenation may significantly influence therapeutic success. In particular, the efficacy of radiotherapy and photodynamic therapy depends on pO_2 . Separate or combined chemotherapeutic approaches have also been proposed, exploiting selective cytotoxicity of bioreductive drugs towards hypoxic cells, and certain drugs may act preferentially under hypoxic conditions. Many techniques for measuring tissue oxygenation have been developed. However, most of them are either invasive or lack of spatial resolution. NMR techniques have the potential advantages of being non-invasive and repeatable, and having high spatial resolution.

Fluorine NMR can provide a direct measurement of pO_2 based on the response of the spin-lattice relaxation rate ($R1 = 1/T1$) of perfluorocarbons (PFCs) to pO_2 *in vivo*. We have surveyed the relative sensitivity of several PFCs and now find HFB offers exceptional sensitivity to changes in pO_2 with relatively little response to temperature. HFB has a single resonance, providing optimal signal-to-noise ratio (SNR). We have now applied this novel technique to investigate dynamic changes in pO_2 in tumors in response to respiratory challenges and the feasibility of mapping the clearance rate of HFB, and compared the results with changes in hemoglobin saturation (sO_2) and concentration in tumor vasculature observed using a new NIR system.

Breast 13762 NF or Dunning prostate R3327-AT1 adenocarcinomas were implanted in skin pedicles on the forebacks of adult female Fischer or male Copenhagen rats (~ 250 g). Once the tumors reached ~ 1cm diameter, the rats were anesthetized with 200 μ l ketamine hydrochloride, intramuscularly and maintained under general gaseous anesthesia with 33% O_2 , 66% N_2O , and 0.5% methoxyflurane. The tumor blood sO_2 was assessed by NIR spectroscopy using a frequency-domain dual wavelength system (758 nm and 782 nm). The tumor blood volume and sO_2 were calculated from the light amplitude.

$$\Delta[Hb]_{total} = -3.63 * \log (A_I/A_C)^{758} + 8.68 * \log (A_I/A_C)^{782} \quad (1)$$

$$\Delta[HbO_2] - \Delta[Hb] = -18.49 * \log (A_I/A_C)^{758} + 21.20 * \log (A_I/A_C)^{782} \quad (2)$$

where A_I is the initial amplitude (amplitude of baseline), A_C is the current amplitude, and L is the optical pathlength between the source and detector.

Once stable baseline measurements were achieved, the inhaled gas was altered to pure oxygen or carbogen (95% O_2 + 5% CO_2) and dynamic changes were observed over a period of two hours. Both the magnitude and rate of change of sO_2 were examined. Following the NIR experiments, 40 μ l HFB were injected directly into both central and peripheral regions of the tumors using a Hamilton syringe with a 32 gauge needle. The animals were placed on its side in a cradle with a thermal blanket to maintain the body temperature at 37°C. A tunable 2 cm $^1H/^{19}F$ single turn solenoid coil was placed around the tumor and MR experiments were performed using the 4.7 T magnet. Tumor dynamic changes in pO_2 were monitored using ^{19}F PBSR-EPI. Regional tumor pO_2 was estimated using the relationship: $pO_2(\text{torr}) = [R1 - 0.074]/0.0016$,

where $R1$ is the spin lattice relaxation rate of HFB. Twenty-three pO_2 maps were produced in 3 hours with respect to respiratory challenges. Clearance (τ) maps were also produced using the EPI images with the longest delays (90 sec).

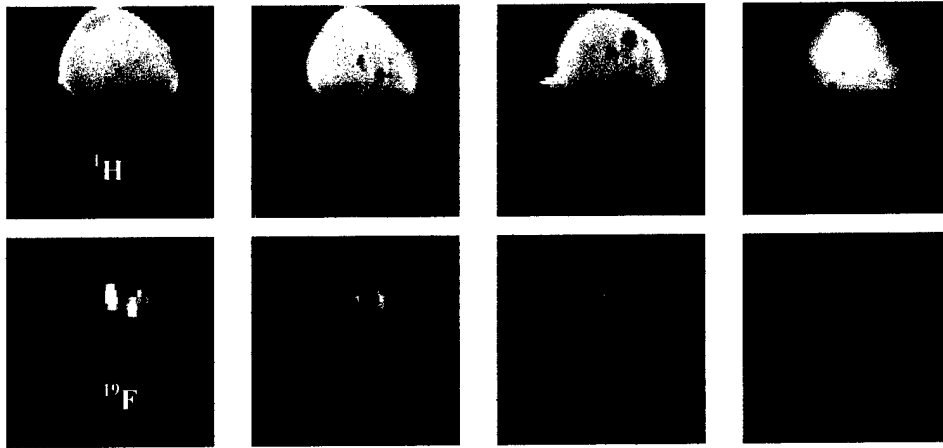


Figure 1. 1H and ^{19}F coronal images of a breast tumor. FOV = 48 x 48 mm, matrix size = 128 x 64, and slice thickness = 4 mm.

Figure 1 shows conventional spin echo (SE) 1H images (top four) and corresponding ^{19}F SE images of a representative breast tumor. 1H images were acquired to show the tumor anatomy and ^{19}F images to show the distribution of HFB within the tumor. Comparison of the 1H and ^{19}F images reveals that the tumor was centrally labeled in this case. For many regions, the HFB signal intensity was found to decay exponentially with a typical biological half-life ranging from $T_{1/2} = 700$ to 1200 min. Since HFB is a non-ionic freely diffusable tracer, we believed that clearance rate would provide an indication of relative tumor blood flow (TBF).

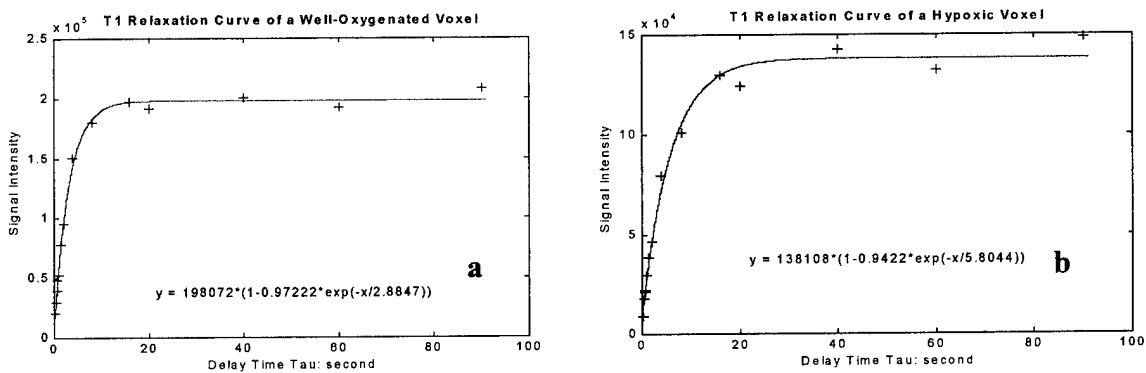


Figure 2. T1 relaxation curves of a well-oxygenated voxel (a) and a hypoxic voxel (b).

Good T1 relaxation curve fit is crucial in ^{19}F PBSR-EPI oximetry. To assess the goodness of curve fit, I wrote a Unix based NMR-shell script program to display the T1 relaxation curves of individual voxels of the PBSR-EPI images. The graphical representation of the data,

relaxation model, and goodness of fit provides a quick and convenient way of assessing the quality of the data. Figure 2 shows T1 relaxation curves of a well-oxygenated voxel (a) and a hypoxic voxel (b).

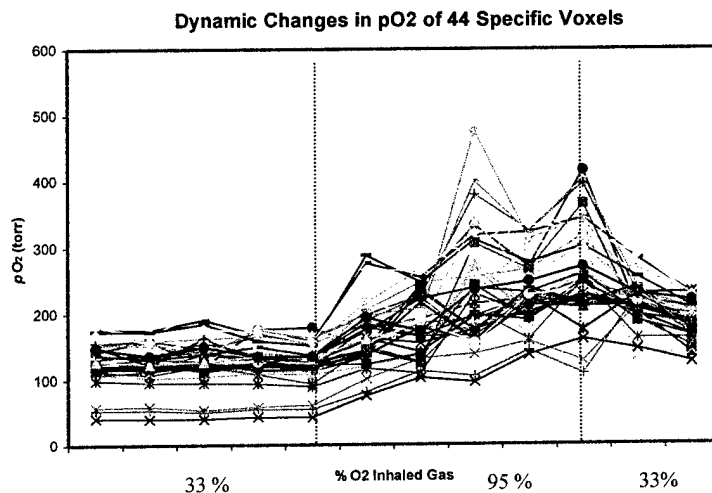


Figure 3. Dynamic changes in pO_2 of 44 specific voxels of a breast tumor.

The ^{19}F MR-EPI oximetry of tumor has the distinct advantage over other techniques that subsequent measurements are completely non-invasive. The greatest strength of this method is the ability to trace the fate of individual voxels (regions) with respect to therapeutic interventions. Figure 3 shows dynamic changes in pO_2 of 44 specific voxels of a breast tumor with respect to different inhaled gases. Error bars have been omitted for the sake of clarity. It is noteworthy that voxels with high baseline pO_2 had significantly different response characteristics from those with initially low pO_2 , which showed small changes. To further investigate the temporal response of individual voxels, we modeled the temporal response in pO_2 using exponential equations:

$$1) y = a + b \cdot (1 - e^{-t/\tau}), \text{ for increasing trend}$$

$$2) y = a + b \cdot e^{-t/\tau}, \text{ for decreasing trend}$$

where y is pO_2 , a and b are two constants, t is time, and τ is the time constant.

We found that the time constants of well-oxygenated voxels (10 ~ 20 min) were much shorter than those of hypoxic voxels (> 50 min) and the global pO_2 time constant (60 ~ 80 min) was much longer than the blood hemoglobin saturation (sO_2) time constant (10 ~ 20 min) (for detailed information regarding the NIR results, please refer to Appendices). NIR showed significant changes in tumor vascular oxygenation accompanying respiratory interventions. ^{19}F MR-EPI showed significant changes in tumor tissue pO_2 , with considerable regional heterogeneity in both absolute values and rate of change accompanying interventions. In general,

changes in tumor vascular sO_2 preceded tumor tissue pO_2 , particularly for smaller tumors. Figure 4 shows the exponential response model of a representative voxel when the inhaled gas was switched from 33% O_2 to carbogen.

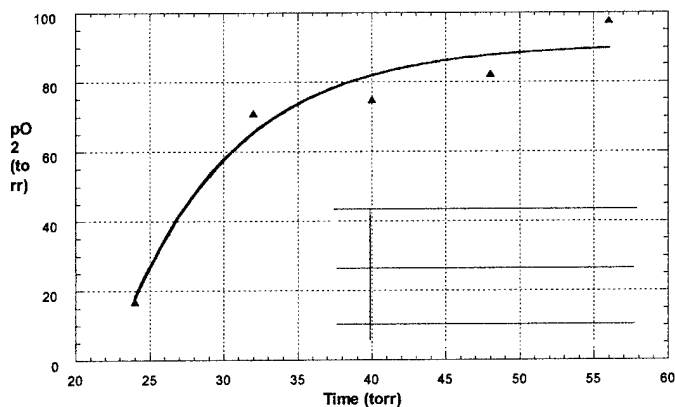


Figure 4. Dynamic response of pO_2 : the time constant τ of a representative voxel.

We also found that strong correlation existed between the maximum pO_2 value (breathing carbogen) attained during the course of an experiment and mean baseline pO_2 ($r^2 = 0.7856$) (Figure 5a) and between mean pO_2 (breathing carbogen) and mean baseline pO_2 ($r^2 = 0.9065$) (Figure 5b).

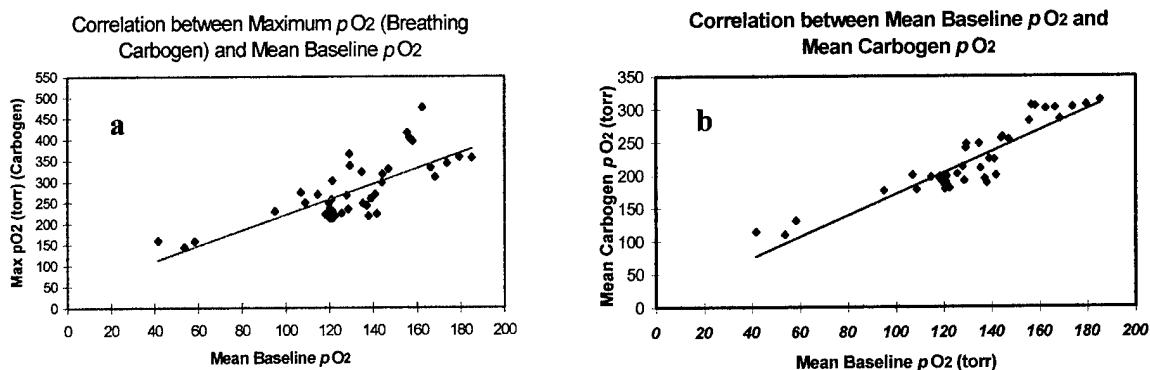


Figure 5. Correlation between maximum pO_2 , mean pO_2 (breathing carbogen) and mean baseline pO_2 .

Currently, I am still in a process of analyzing the data. However, preliminary results indicate that this method offers several distinct advantages: 1) requisite precision of pO_2 determinations; 2) ability to interrogate selected tumor regions; 3) high temporal resolution; 4) low sensitivity to temperature; and 5) small volumes of reporter molecule. Now, I am building new RF coils that allow us to measure tumor tissue pO_2 using ^{19}F MR-EPI and vascular sO_2 using NIR spectroscopy simultaneously. This technique will further enhance our understanding of tumor physiology and response to therapy.

IV. APPENDICES

1. A List of Key Research Accomplishments

- The HFB signal intensity was found to decay exponentially with a typical biological half-life ranging from $T_{1/2} = 700$ to 1200 min, which, we believe, would provide an indication of relative tumor blood flow (TBF).
- Tumor voxels with high baseline pO_2 had significantly different response characteristics from those with initially low pO_2 , with voxels of high baseline pO_2 showing significant changes in pO_2 while voxles of low baseline pO_2 showing small changes.
- Time constants (τ) of well-oxygenated voxels (10 ~ 20 min) were much shorter than those of hypoxic voxels (> 50 min). The global pO_2 time constant (60 ~ 80 min) was much longer than the blood hemoglobin saturation (sO_2) time constant (10 ~ 20 min).
- NIR spectroscopy showed significant changes in tumor vascular oxygenation (sO_2) accompanying respiratory interventions. ^{19}F MR-EPI showed significant changes in tumor tissue pO_2 , with considerable regional heterogeneity in both absolute values and rate of change accompanying interventions. Changes in tumor vascular sO_2 preceded tumor tissue pO_2 , particularly for smaller tumors.
- Strong correlation existed between the maximum pO_2 value attained during the course of an experiment and mean baseline pO_2 ($r^2 = 0.7856$) and between mean pO_2 and mean baseline pO_2 ($r^2 = 0.9065$).
- ^{19}F EPI oximetry of HFB was proven to be a useful technique for measuring tumor oxygenation.
- pO_2 and the distribution of pO_2 in breast 13762 NF and Dunning prostate R3327-AT1 adenocarcinomas changed with tumor growth and there existed heterogeneity in pO_2 distribution.
- Tumor oxygenation could be manipulated by inhaling different gases.

2. A List of Reportable Outcomes

Manuscripts:

- 1) **"Tumor Oximetry: A Comparison between Near-infrared Frequency-Domain Spectroscopy of Hemoglobin Saturation and ^{19}F MRI of Hexafluorobenzene"**
Katherine L. Worden, **Yulin Song**, Xin Jiang, Anca Constantinescu, Ralph P. Mason, and Hanli Liu
(Presented at the International Symposium on Biomedical Optics, sponsored by the Society of Photo-Optical Instrumentation Engineers (SPIE), 1998, in press).
- 2) **"Tumor Oximetry: Comparison of ^{19}F MR EPI and Electrodes"**
Ralph P. Mason, Sandeep Hunjan, Anca Constantinescu, **Yulin Song**, Dawen Zhao, Eric W. Hahn, Peter P. Antich, and Peter Peschke
(Presented at the 27th Annual Meeting of International Society on Oxygen Transport to Tissue (ISOTT), 1999, in press).

Abstracts:

- 1) **"Regional Tumor Oxygen Tension and Blood Flow: Correlation Studies Using ^{19}F PBSR-EPI of Hexafluorobenzene"**
Yulin Song, Ralph P. Mason, Sandeep Hunjan, Anca Constantinescu, Eric Hahn, and Peter Antich
(Presented at the Workshop on Magnetic Resonance in Experimental and Clinical Cancer Research, sponsored by the International Society for Magnetic Resonance in Medicine (ISMRM), 1998).
- 2) **"Tumor Oxygen Dynamics: Comparison between ^{19}F MR-EPI of Hexafluorobenzene and Frequency Domain NIR Spectroscopy"**
Yulin Song, Kate L. Worden, Xin Jiang, Dawen Zhao, Anca Constantinescu, Hanli Liu, and Ralph P. Mason
(Presented at the 27th Annual Meeting of International Society on Oxygen Transport to Tissue (ISOTT), 1999).
- 3) **"Tumor Oxygenation and Measurement of Regional Dynamic Changes"**
Ralph P. Mason, Sandeep Hunjan, Anca Constantinescu, **Yulin Song**, Eric W. Hahn, Peter P. Antich, Christian Blum, and Peter Peschke
(Presented at International Conference on Molecular Determinants of Sensitivity to Antitumor Agents, sponsored by American Association for Cancer Research (AACR), 1999).

3) Copies of Manuscripts and Abstracts

Tumor Oximetry: A comparison between near-infrared frequency-domain spectroscopy of hemoglobin saturation and ¹⁹F MRI of hexafluorobenzene

Katherine L. Worden^{*}, Yulin Song^{* ϕ} , Xin Jiang^{*}, Anca Constantinescu ^{ϕ} , Ralph P. Mason ^{ϕ} , Hanli Liu^{*}

^{*}Joint Biomedical Engineering Program
University of Texas at Arlington/University of Texas Southwestern Medical Center at Dallas
Dallas, TX 75235

^{ϕ} Department of Radiology
University of Texas Southwestern Medical Center at Dallas
Dallas, TX 75235

ABSTRACT

Studies have shown that hypoxic tumor cells are relatively more resistant to radiotherapy, chemotherapy, and photodynamic therapy. Tumor oximetry, e.g., measurement of oxygen tension (pO₂) of tissue and/or blood oxygenation (SO₂) of the vascular bed, could be valuable for optimizing treatment plans.

In this study, we employed a recently developed homodyne system to measure changes in hemoglobin saturation (SO₂) and concentration in the vascular bed of rat prostate and breast tumors. For comparison, tissue pO₂ values were measured using ¹⁹F MR EPI of hexafluorobenzene, providing a map of regional tumor oxygenation tension. Both SO₂ and pO₂ measurements were taken while the inhaled gas was alternated between 33% oxygen, 100% oxygen and carbogen (95% oxygen, 5% CO₂).

The results obtained for both techniques showed significant changes in tumor oxygenation accompanying respiratory challenge, with changes in vascular SO₂ preceding tissue pO₂ change. The combined use of these two techniques provides new insight into the dynamics of tumor oxygenation by making available a method of obtaining regional information of the state of the tissue, as well as a non-invasive, real-time method for determining changes in the vascular bed.

Keywords: Frequency-Domain Spectroscopy, NIR spectroscopy, ¹⁹F MRI, Hexafluorobenzene, Oximetry

1. INTRODUCTION

Frequently, blood vessel formation is unable to keep up with the rapid growth of a tumor. If this occurs, the cells in the tumor furthest from a fresh blood supply will suffer a lack of oxygen and hypoxic areas will form (chronic hypoxia). These regions can be as much as 3 times more resistant to radiotherapy.¹ In addition to studies in vitro and in animal tumors, there is increasing evidence from clinical trials that poorly oxygenated tumors indicate poor prognosis for patients.^{2,3} Methods of determining the oxygen content of a tumor could, therefore, be helpful in the development of an optimal treatment plan. This paper will present the experimental results of two such methods: NIR spectroscopy to determine blood oxygenation (SO₂) of the tumor's vascular bed and ¹⁹F MRI of hexafluorobenzene (HFB) to determine tissue pO₂.

NIR spectroscopy, through use of a recently developed frequency-domain system, based on an in-phase and quadrature (IQ) demodulator chip⁴, is attractive as a non-invasive, inexpensive, portable, real-time system that can provide global SO₂ values. We show that this IQ system can be used to determine the SO₂ in a tumor's vascular bed and measure the

response of blood volume and oxygen saturation to inhaled gas. The technique of using ^{19}F MRI relaxometry to map tissue $p\text{O}_2$ is also relatively new.⁵ The spin-lattice relaxation rate of hexafluorobenzene is particularly sensitive to oxygen while being insensitive to temperature.⁶ Following direct injection of HFB into a tumor, ^{19}F MRI maps tissue $p\text{O}_2$ at millimeter resolution. This method facilitates measurements of dynamic changes in $p\text{O}_2$ accompanying therapeutic interventions and allows the fate of individual voxels to be traced.

Through comparison of these two techniques, it is possible to examine the relationship between SO_2 of the vascular bed and $p\text{O}_2$ of the tissue. Blood oxygenation, blood volume, arterial SO_2 and temperature may also be compared.

2. METHODS AND INSTRUMENTATION

2.1 Tumor Model

Dunning prostate adenocarcinoma R3327-AT1 was implanted in adult male Copenhagen rats and NF13762 breast tumor in female Fisher rats. The tumors were grown in pedicles⁷ on the forebacks of the rats until they were approximately 2 cm in diameter. Rats were anesthetized with 200 μl ketamine hydrochloride (100 mg/ml) and maintained under general gaseous anesthesia with 33 % inhaled O_2 [0.3 dm^3/min O_2 , 0.6 dm^3/min N_2O , and 0.5% methoxyflurane] through a mask placed over the mouth and nose. Body temperature was maintained by a warm water blanket. A fiber optic pulse oximeter was placed on the hind foot to monitor arterial oxygenation (A_{SO_2}) and a fiber optic probe was inserted rectally to measure temperature. Inhaled gas was alternated between 33% oxygen, 100% oxygen and carbogen (95% oxygen, 5% carbon dioxide). NIR and EPI measurements were performed sequentially for comparison.

2.2 NIR Spectroscopy

As shown in figure 1, we used a new homodyne system able to determine amplitude and phase changes of light.⁴ In this setup, an RF source modulates the light from two laser diodes (wavelengths 758 nm and 782 nm) at 140 MHz. The light passes through fiber optic cables, is transmitted through the tumor tissue, and is collected by a second fiber bundle. The light is then detected by a PMT and is demodulated with a commercially available in-phase and quadrature (IQ) demodulator chip into I and Q components. Once these components are put through a low pass filter, they can be used to calculate amplitude and phase changes caused by the tumor. These steps can be seen mathematically in equations 1-4.

$$(1) \quad I(t) = 2A \sin(\omega t + \theta) \sin(\omega t) = A \cos(\theta) - A \cos(\omega t + \theta) \quad \text{---> low pass filter --->} \quad I_{\text{dc}} = A \cos(\theta)$$

$$(2) \quad Q(t) = 2A \sin(\omega t + \theta) \cos(\omega t) = A \sin(\theta) + A \sin(\omega t + \theta) \quad \text{---> low pass filter --->} \quad Q_{\text{dc}} = A \sin(\theta)$$

$$(3) \quad \theta = \tan^{-1}(Q_{\text{dc}} / I_{\text{dc}})$$

$$(4) \quad A = (I_{\text{dc}}^2 + Q_{\text{dc}}^2)^{1/2}$$

A = amplitude of detected light; θ = phase of detected light; ω = modulation frequency (140 MHz)

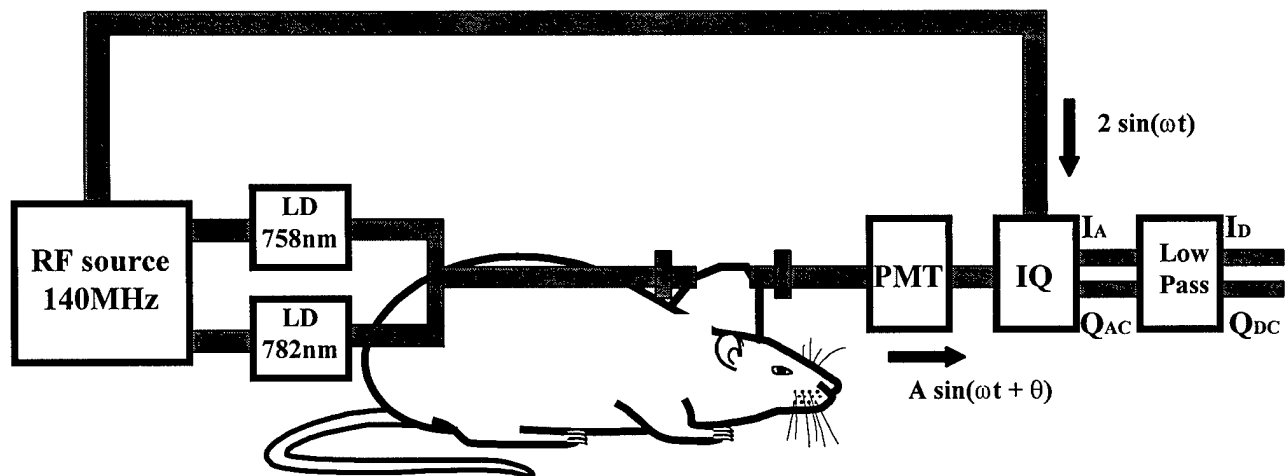


Figure 1: Setup for NIR experiment.

NIR spectroscopy can be used to determine hemoglobin saturation because the extinction coefficient values of deoxygenated hemoglobin differ from those of oxygenated hemoglobin at the wavelengths selected (758 nm and 782 nm). At this point in our algorithm calculations, we have assumed background absorbance to be negligible and estimated that the absorption coefficients were composed of the extinction coefficients for deoxy-hemoglobin and oxy-hemoglobin multiplied by their respective concentrations (equations 5&6).

$$(5) \quad \mu_a^{758} = \epsilon_{Hb}^{758}[Hb] + \epsilon_{HbO_2}^{758}[HbO_2]$$

$$(6) \quad \mu_a^{782} = \epsilon_{Hb}^{782}[Hb] + \epsilon_{HbO_2}^{782}[HbO_2]$$

The IQ system does give both phase and amplitude values, but given the tumor's small size and our fiber configuration, we haven't yet derived a suitable algorithm to compute μ_a and μ_s . The data presented in this paper were analyzed using Beer-Lambert's law and the amplitude values to find trends in the changing absorption coefficients (equation 7). By manipulating equations 5-7, we can calculate changes in blood volume and saturation from the transmitted amplitude of the light through the tumor (equations 8&9).

$$(7) \quad \mu_{aC} - \mu_{aI} = 1/L * \log(A_I/A_C)$$

$$(8) \quad \Delta[Hb]_{total} = -3.63 * \log(A_I/A_C)^{758} + 8.68 * \log(A_I/A_C)^{782}$$

$$(9) \quad \Delta[HbO_2] - \Delta[Hb] = -18.49 * \log(A_I/A_C)^{758} + 21.20 * \log(A_I/A_C)^{782}$$

A_I = initial amplitude (amplitude of baseline); A_C = current amplitude; L = optical pathlength between source/detector; The constants were computed with extinction coefficients for oxy- and deoxy- hemoglobin at the two wavelengths used.

2.3 MRI Instrumentation and Procedure

MRI experiments were performed on an Omega CSI 4.7 T 40 cm system with actively shielded gradients. A homebuilt tunable $^1H/^{19}F$ single turn solenoid coil was placed around the tumor. HFB (40 μ l) was administered directly into the tumor using a fine sharp (32 G) needle with deliberate dispersion along several tracks to interrogate both central and peripheral tumor regions. HFB is ideal for the imaging of pO_2 because it has a single resonance and its relaxation rate varies linearly with oxygen concentration. 1H images were acquired for anatomical reference using a traditional 3D spin-echo pulse sequence as seen in **figure 2a**. Conventional ^{19}F MR images (**figure 2b**) were then taken to show the 3D distribution of the HFB in the tumor. **Figure 2b** may be directly overlaid over **figure 2a** to show the position of the HFB in that slice.

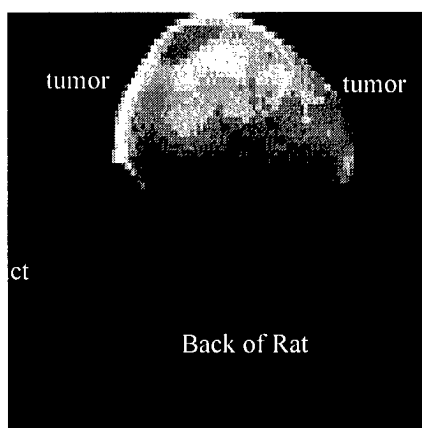


Figure 2a: Proton (1H) coronal image of a representative slice through a breast tumor (NF13762): TR = 250 ms, TE = 8 ms, NA = 2, FOV = 48 x 48 mm, slice thickness = 4 mm, and matrix size = 128 x 64 x 8.

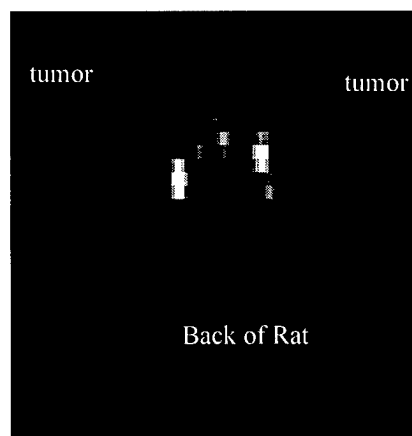


Figure 2b: Corresponding ^{19}F MR Image showing distribution of HFB within the tumor: TR = 150 ms, TE = 8 ms, FOV = 48 x 48 mm, matrix size = 128 x 64x8.

Tumor oxygenation was assessed using ^{19}F PBSR-EPI of HFB.⁸ The PBSR preparation pulse sequence consists of a series of 20 non-spatially selective saturating 90° pulses with 20 ms spacing to saturate the ^{19}F nuclei. Following a variable delay time τ , a single spin echo EPI sequence with “blipped” phase encoding was applied.⁹ A PBSR-EPI image corresponding to the images shown in **figures 2a and 2b** is shown in **figure 2c**. Fourteen 32×32 PBSR-EPI images, with τ ranging from 200 ms to 90 sec and an FOV of 40×40 mm, were acquired in eight minutes. An $R1$ map was obtained by fitting signal intensity of each voxel of the fourteen images to a three parameter relaxation model by Levenberg-Marquardt least squares algorithm (equation 10):

$$(10) \quad y_n(i, j) = A(i, j) \cdot [1 - (1 + W) \cdot \exp(-R1(i, j) \cdot \tau_n)]$$

$$(n = 1, 2, \dots, 14)$$

$$(i, j = 1, 2, \dots, 32)$$

where $y_n(i, j)$ is the measured signal intensity corresponding to delay time τ_n (the n th images) for voxel (i, j) , $A(i, j)$ is the fully relaxed signal intensity amplitude of voxel (i, j) , W is a dimensionless scaling factor allowing for imperfect signal conversion, and $R1(i, j)$ is the relaxation rate of voxel (i, j) in unit of sec^{-1} . A , W and $R1$ are the three fit parameters.

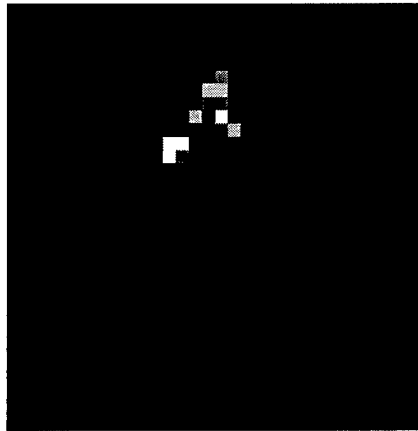


Figure 2c: ^{19}F PBSR-EPI projection image obtained from the tumor in **figure 1** in a single acquisition ($\tau = 90$ s). Fourteen images were acquired with variable relaxation delays (τ) ranging from 200 ms to 90 sec. Using a 32×32 matrix, FOV of 40×40 mm, $p\text{O}_2$ maps were generated with 1.25×1.25 mm resolution.

$p\text{O}_2$ maps were then generated by applying the calibration curve: $p\text{O}_2(\text{torr}) = [R1(\text{s}^{-1}) - 0.074] / 0.0016$ to the $R1$ maps.¹⁰ The map shown in **figure 2d** focuses on a region of the same slice that was presented in figures 2a-2c.

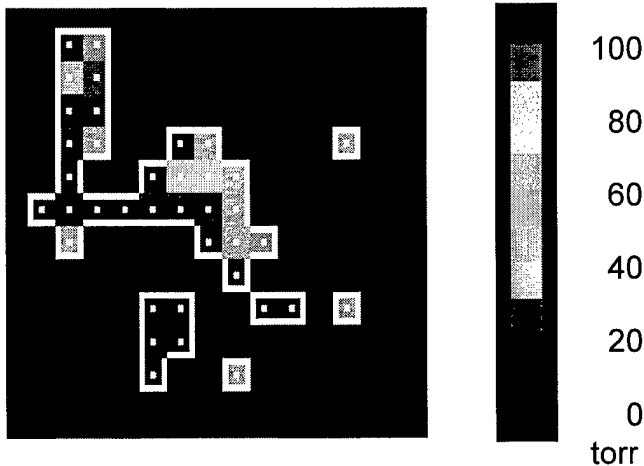


Figure 2d: Typical $p\text{O}_2$ map, composed of fourteen PBSR images from the tumor presented in **figure 2a-c**. Using a 32×32 matrix, FOV of 40×40 mm, $p\text{O}_2$ maps were generated with 1.25×1.25 mm resolution.

3. RESULTS

3.1 NIR Results

The effects of the inhaled gas on hemoglobin saturation and concentration, as recorded by the IQ system, are shown below in **figures 3a & 3b**. The X-axis shows time in minutes from the start of the experiment and the dotted vertical lines mark the point when the gas was changed. Hemoglobin saturation and concentration are presented as unit-less, relative trends. It can easily be seen that hemoglobin saturation begins to increase almost immediately after a gas switch from baseline (33% oxygen) to either carbogen or 100% oxygen and increases steadily for several minutes. Total hemoglobin change is quite small in comparison, indicating relatively constant blood volume in the tumor. These trends seem fairly consistent for both breast and prostate tumors. Typical responses of a breast tumor and prostate tumor are presented in **figures 3a & 3b**, respectively.

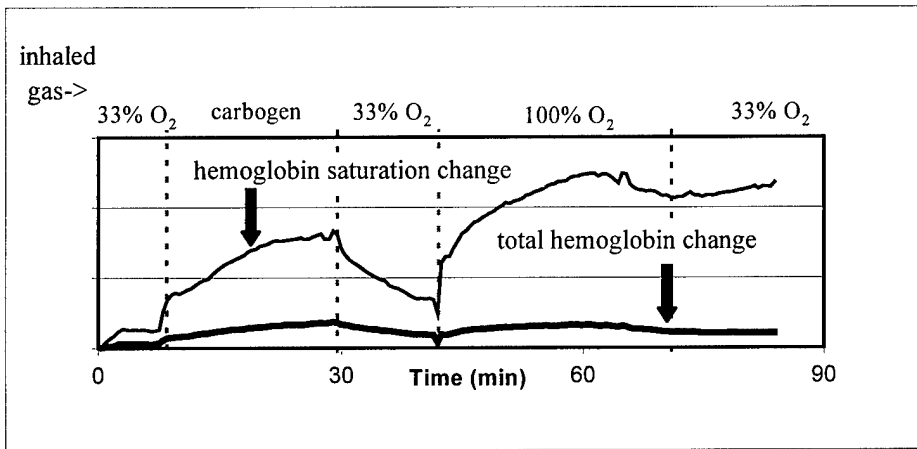


Figure 3a: Hemoglobin saturation and concentration change in a breast tumor.

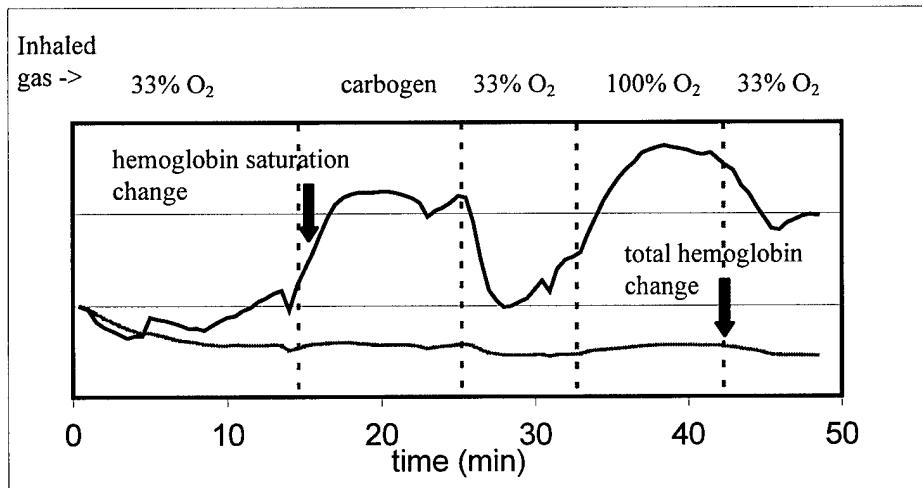


Figure 3b: Hemoglobin saturation and concentration change in a prostate tumor.

It is also worthwhile to compare the saturation changes measured in the tumors vascular bed by the IQ system with the arterial saturation changes measured by a pulse oximeter from the rat's hind foot. One such comparison taken from a prostate tumor is presented below as **figure 4**. Hemoglobin saturation in the vascular bed is again represented as a unit-less trend and arterial saturation values are presented to the right. Again, the X-axis gives the time from the beginning of the experiment in minutes and the dotted lines mark the time of gas change. In this case, the arterial saturation follows the same trend as the tumor vascular bed's hemoglobin saturation, but shows a faster change. Such close similarity wasn't always observed.

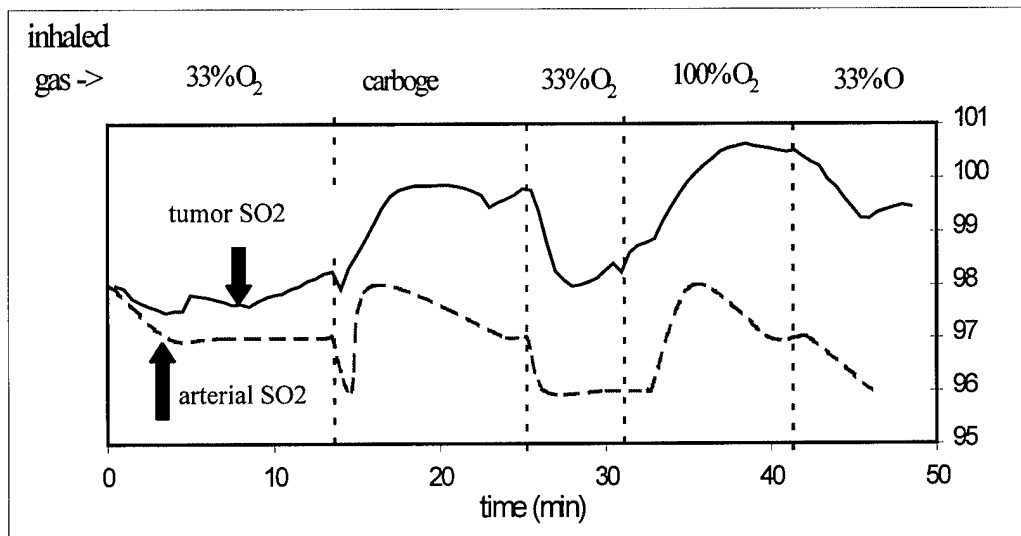


Figure 4: In the prostate tumor presented in Figure 4, both arterial SO₂ and the SO₂ in the tumor increased for inhaled carbogen and 100% O₂ and decreased for 33% O₂. Arterial SO₂ in hind foot measured by a commercial pulse oximeter and SO₂ in tumor using IQ system.

3.2 MRI Results

MRI provides the advantage of being able to look at regional changes in pO₂ values. Histograms, such as those presented in **figure 5**, are able to show the heterogeneity of pO₂ values within the tumor as well as the average pO₂ values. The data presented here were taken from a breast tumor and show the average values from the data of several pO₂ maps that were taken throughout the administration of each gas. In **figure 5a**, we see that when the rat was breathing 33% oxygen, the average pO₂ value was about 40 torr. When the rat was breathing carbogen (**figure 5b**), there was a large shift towards higher pO₂ values leading to a mean value of about 99 torr. These values increased further while the rat was breathing 100% oxygen (**figure 5c**) such that the average voxel now had a pO₂ value of about 145 torr. The time course of these changes is presented later in the paper in **figure 7b**.

Figure 5a:
 pO₂ range while the rat was breathing
 33% oxygen.
 Average value = 40 ± 3 torr

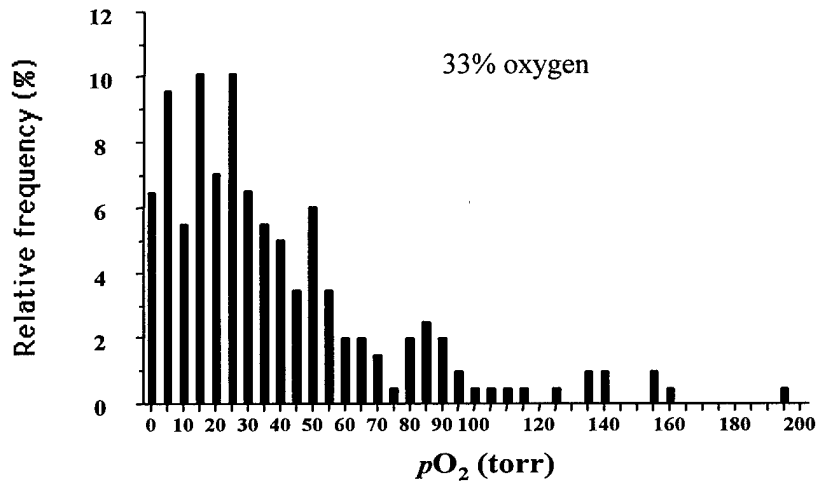


Figure 5b:
 pO₂ range while the rat was breathing
 carbogen.
 Average value = 99 ± 4 torr

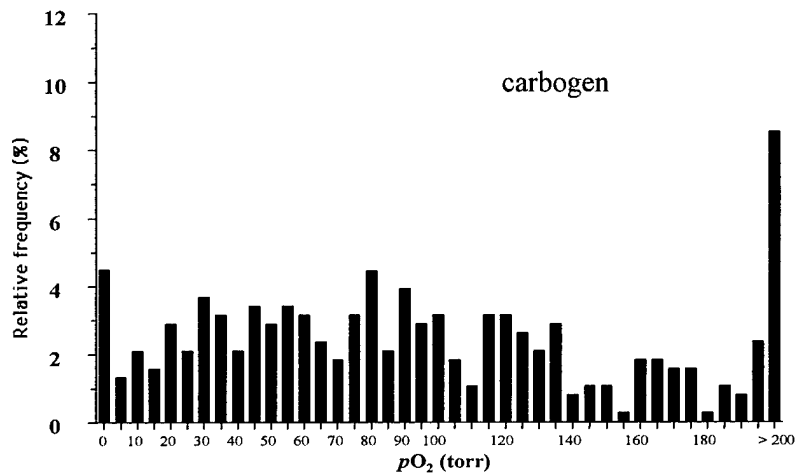
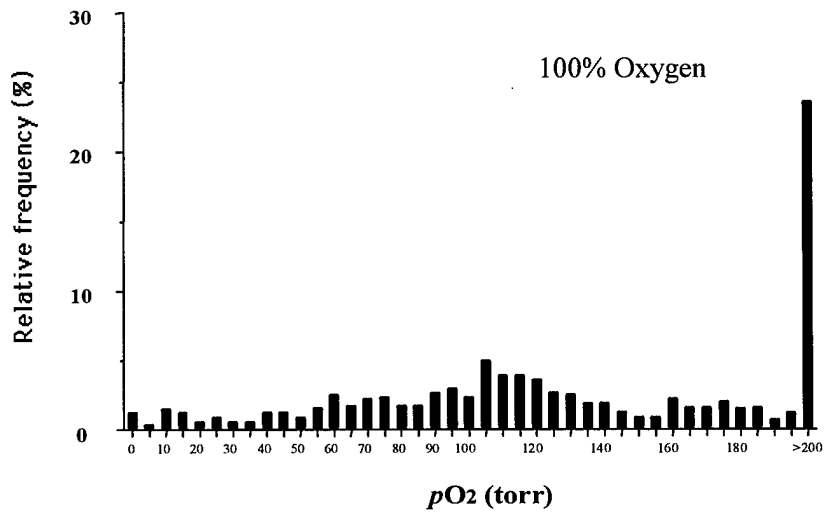


Figure 5c:
 pO₂ range while the rat was breathing
 100% oxygen.
 Average value = 145 ± 4 torr



3.3 Comparison

While absolute pO_2 values are important for investigating hypoxia, dynamic changes may be more interesting for investigation of response to intervention. In figures 6 & 7, the dynamic changes in pO_2 and SO_2 are compared. These plots show that pO_2 reacts in a very similar fashion to blood saturation, but that the effect is slower. Since the IQ system provides a global measure across the whole tumor, pO_2 measurements are presented here as mean values attained from the pixels of each pO_2 map. The NIR and MRI data shown are for the same rat undergoing the same procedure, but on consecutive days. Data from two breast tumors of various size are presented. The larger tumor was about 2.1 x 2.4 x 2.2 cm whereas the smaller tumor was 1.9 x 2.2 x 2 cm. Inhaling carbogen and 100% oxygen each consistently resulted in increased SO_2 and pO_2 over 33% oxygen. The pO_2 and SO_2 measurements were plotted against the same X-axis to allow rate of change to be compared.

Figure 6a: Saturation from IQ

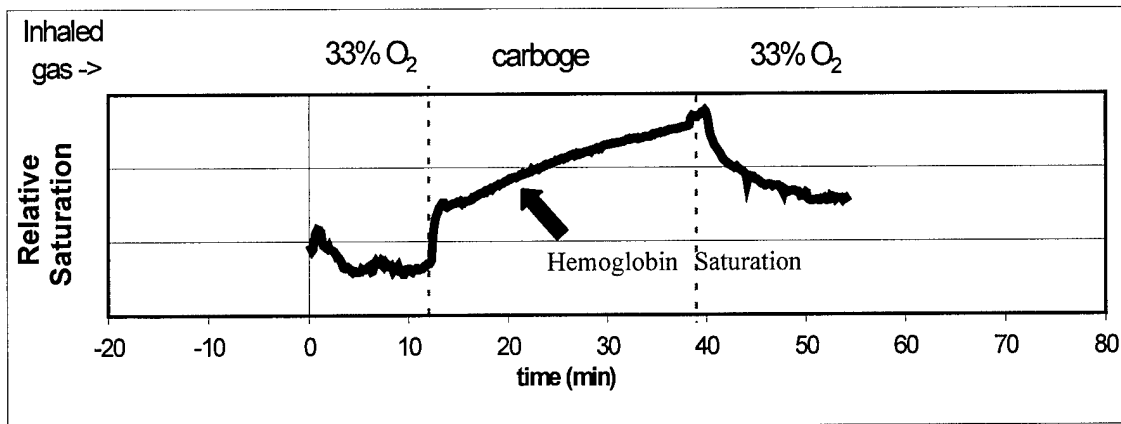


Figure 6b: pO_2 from MRI

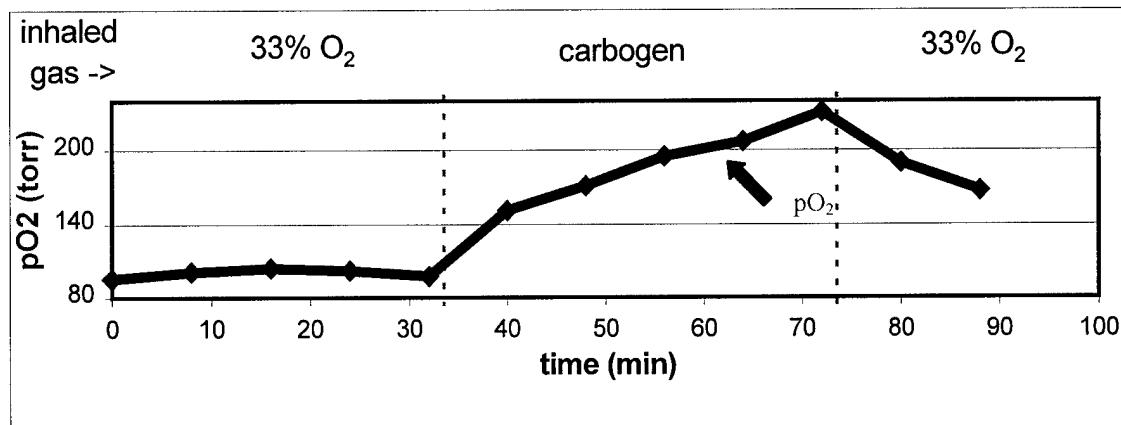


Figure 6: These two sets of data were taken from the small rat breast tumor on consecutive days. Both the pO_2 and blood saturation increased with a transition from 33% to carbogen, and decreased when switched back to 33%.

Figure 7a: Saturation from IQ

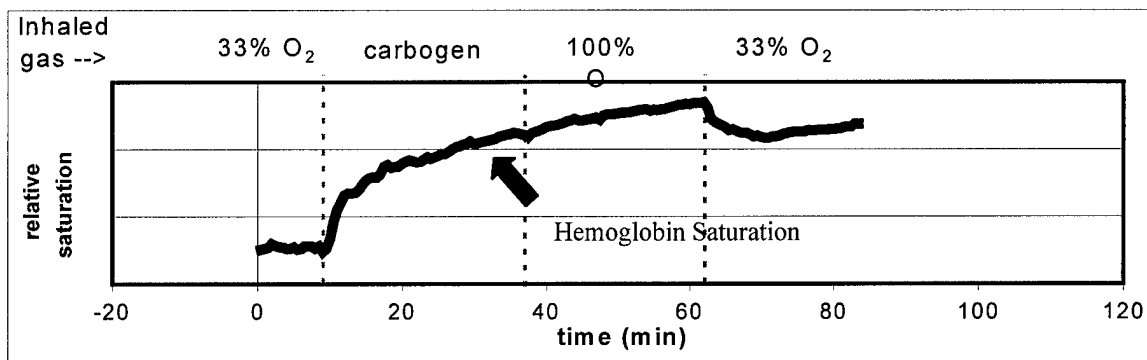


Figure 7b: pO₂ from MRI

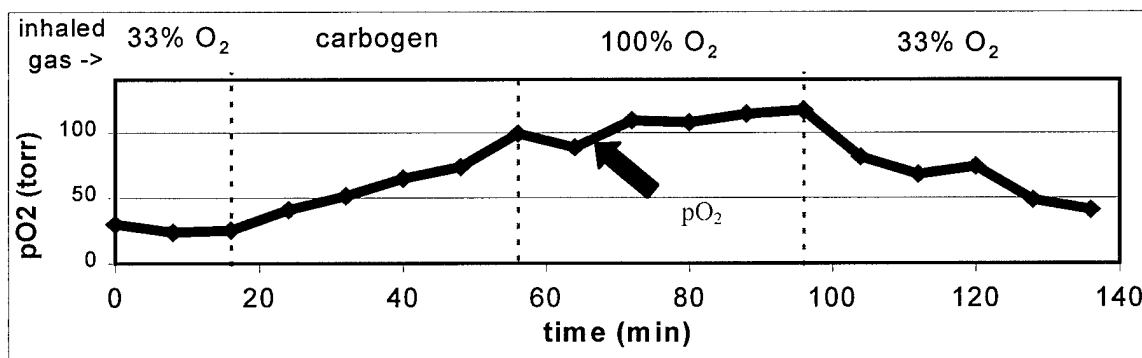


Figure 7: These two sets of data were taken from the large rat breast tumor on consecutive days. Both the pO₂ and blood saturation increased with a transition from 33% to carbogen, and then further increased slightly when switched from carbogen to 100% oxygen. Values began to decrease when switched back to 33%.

To further study the temporal response, the changes in pO₂ and SO₂ were modeled using the exponential equations 11 and 12. A non-linear curve fitting method was used to obtain τ .

(11) For increasing values: $\text{Saturation} = a + b \cdot (1 - e^{-t/\tau})$

(12) For decreasing values: $\text{Saturation} = a + b \cdot (e^{-t/\tau})$

Generally, blood saturation effects had a much shorter time constant than oxygen tension in the tissue (Figure 8). For the larger tumor, the rate of increase and decrease were much faster for SO₂ than pO₂. Less difference was seen in the smaller tumor. Further study for confirmation is underway.

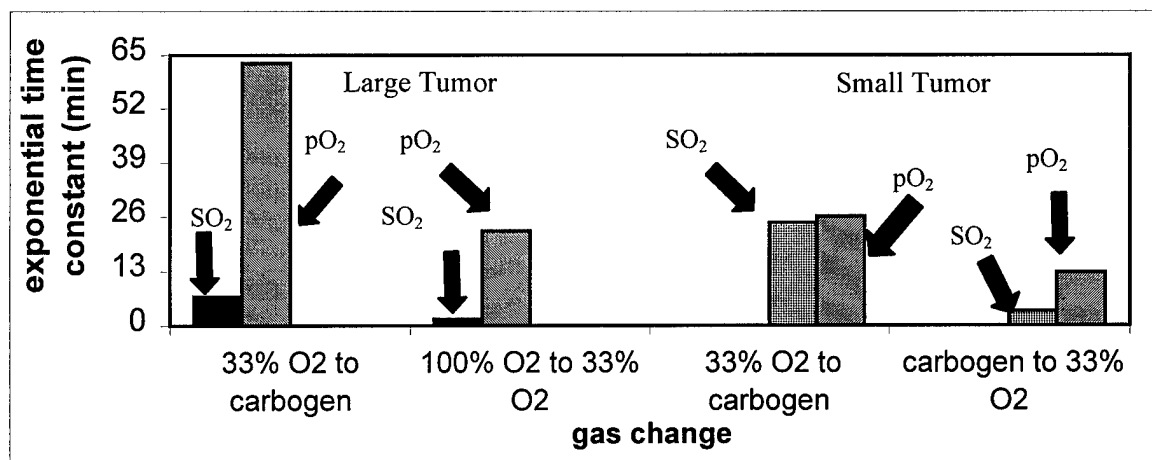


Figure 8: Time constants for the data presented in Figures 6&7.

4. CONCLUSION

The data suggest interesting correlations between several physiological parameters. Both tumor vascular Hb saturation and mean pO₂ increased in response to inhaling an elevated percent O₂, either through carbogen or 100% O₂. Arterial SO₂ and tumor SO₂ respond similarly to changes in inhaled gas, with arterial changes preceding changes in the tumor vascular bed. Changes in SO₂ are generally faster than pO₂, though absolute values are highly variable and suggest heterogeneity amongst the tumor population. Given the distinct heterogeneity among tumors even of a given type and size,¹¹ further investigations are required to form a sound picture of the interplay of multiple physiological parameters.

ACKNOWLEDGEMENTS

This work was supported in part by The Whitaker Foundation (HL, RPM), The American Cancer Society RPG-97-116-010CCE (RPM), and the Department of Defense Breast Cancer Initiative BC962357 (YS). MRI experiments were performed at the Mary Nell & Ralph B. Rogers MR Center, an NIH BRTP Facility no. 5-P41-RR02584. We are very grateful to Sandeep Hunjan for assistance with data analysis.

REFERENCES

- ¹ Denekamp, J. Physiological hypoxia and its influence on radiotherapy. *The Biological Basis of Radiotherapy, Second Edition*, Eds. G.G. Steel, G.E. Adams & A. Horwich (Elsevier Science Publishers B.V., 1989)
- ² M. Höckel, K. Schlenger, B. Aral, M. Mitze, U. Schäffer and P. Vaupel, Association between tumor hypoxia and malignant progression in advanced cancer of the uterine cervix. *Cancer Res.* **56**, 4509-15 (1996).
- ³ A.W. Fyles, M. Milosevic, R. Wng, M.C. Kavanagh, M. Pintile, A. Sun, W. Chapman, W. Levin, L. Manchul, T.J. Keane and R. P. Hill, Oxygenation predicts radiation response and survival in patients with cervix cancer. *Radiother. Oncol.* **48**, 149-56 (1998).
- ⁴ Y. Yunsong, H. Liu, X. Li, B. Chance, Low-cost frequency-domain photon migration instrument for tissue spectroscopy, oximetry, and imaging. *Opt. Eng.* **36**(5) 1562-1569 May 1997
- ⁵ R. P. Mason, Non-invasive physiology: ¹⁹F NMR of perfluorocarbon. *Art. Cells, Blood Sub. & Immob. Biotech.* **22**, 4, 1141-1153 (1994).
- ⁶ R.P. Mason, W. Rodbumrung and P.P. Antich, Hexafluorobenzene: a sensitive ¹⁹F NMR indicator of tumor oxygenation. *NMR in Biomed.* **9**, 125-134 (1996).
- ⁷ E. W. Hahn, P. Peschke, R. P. Mason, E. E. Babcock and P. P. Antich, Isolated tumor growth in a surgically formed skin pedicle in the rat: a new tumor model for NMR studies. *Magn. Reson. Imaging* **11**, 1007-1017 (1993).
- ⁸ D. Le, R. P. Mason, S. Hunjan, A. Constantinescu, B. R. Barker and P. P. Antich, Regional tumor oxygen dynamics: ¹⁹F PBSR EPI of hexafluorobenzene. *Magn. Reson. Imaging* **15**, 8, 971-81 (1997).
- ⁹ B. R. Barker, R. P. Mason, N. Bansal and R. M. Peshock, Oxygen tension mapping by ¹⁹F echo planar NMR imaging of sequestered perfluorocarbon. *JMRI* **4**, 595-602 (1994).
- ¹⁰ D. Le, R. P. Mason, S. Hunjan, A. Constantinescu, B. R. Barker and P. P. Antich, Regional tumor oxygen dynamics: ¹⁹F PBSR EPI of hexafluorobenzene. *Magn. Reson. Imaging* **15**, 8, 971-81 (1997).
- ¹¹ R. P. Mason, A. Constantinescu, S. Hunjan, D. Le, E. W. Hahn, P. P. Antich, C. Blum and P. Peschke, Regional tumor oxygenation and measurement of dynamic changes. *Radiat. Res.* (submitted 1998).

TUMOR OXIMETRY: COMPARISON OF ^{19}F MR EPI AND ELECTRODES

Ralph P. Mason, Sandeep Hunjan, Anca Constantinescu, Yulin Song, Dawen Zhao,
Eric W. Hahn, Peter P. Antich, and Peter Peschke⁺.

U.T. Southwestern Medical Center, Dallas, TX and ⁺DKFZ, Heidelberg, Germany

*address correspondence to:

Ralph P. Mason, Ph.D., C. Chem.,

Department of Radiology,

U.T. Southwestern Medical Center,

5323 Harry Hines Blvd.,

Dallas, TX 75235-9058

Tel: (214) 648-8926

Fax (214) 648-2991

E. mail: Ralph.Mason@email.swmed.edu

ABSTRACT

We recently described a novel approach to measuring regional tumor oxygen tension using ^{19}F pulse burst saturation recovery NMR echo planar imaging relaxometry of hexafluorobenzene. We have now compared oxygen tension measurements in a group of size matched Dunning prostate rat tumors R3327-AT1 made using this FREDOM (Fluorocarbon Relaxometry using Echo planar imaging for Dynamic Oxygen Mapping). approach with a traditional polarographic method: the Eppendorf Histogram. We also compare MR and electrode approaches to monitoring dynamic changes with respect to interventions and demonstrate extension of the MR technique to rat breast tumors.

Key words: echo planar imaging, electrode, MRI, oxygen, prostate, tumor

Abbreviations ARDVARC (Alternated Relaxation Delays with Variable Acquisitions to Reduce Clearance effects); EPI (echo planar imaging); FREDOM (Fluorocarbon Relaxometry using Echo planar imaging for Dynamic Oxygen Mapping); HFB (hexafluorobenzene); i.t (intra tumoral)

Acknowledgments

This work was supported in part by The American Cancer Society (RPG-97-116-010CCE; RPM), DOD Breast Cancer initiative (YS), Verein zur Forderung der Krebserkennung and Krebsbehandlung e.V. Heidelberg (PP) and the NIH BRTP Facility #5-P41-RR02584.

Introduction

It is widely appreciated that tumor oxygenation may significantly influence therapeutic success. In particular, the efficacy of radiotherapy [1], photodynamic therapy [2] and hypoxia selective chemotherapeutic agents [3] depend on pO_2 . It had been suggested that the ability to measure tumor oxygenation in patients could allow therapy to be individualized and optimized [4], and indeed, several recent studies have found significant prognostic value based on the Eppendorf Histogram in assessing clinical tumors [5-7]. While electrodes may be considered a "gold standard", they have certain shortcomings and there is clearly a need for alternative methods [8]. We have been developing a new approach based on ^{19}F NMR of perfluorocarbons [9-12] and believe the method can now provide useful measurements of tumor oxygen dynamics *in vivo*.

The FREDOM approach exploits the exceptional response of the ^{19}F NMR spin lattice relaxation rate, R_1 , of fluorocarbons to changes in oxygen tension. Fluorocarbons act as ideal liquids and solvation of gases is directly proportional to the partial pressure of the gas (Henry' law). Since oxygen (O_2) is paramagnetic it induces relaxation in solution directly proportional to the concentration of oxygen, and hence, pO_2 [13]. The highly hydrophobic nature of fluorocarbons ensures both a high solubility of gases, providing molecular amplification, and minimal solvation of other materials (*e.g.*, metal ions) minimizing interference from other environmental factors. We, and others, have explored the use of numerous PFC reporter molecules and various routes of administration [14]. We believe that direct intra tumoral (*i.t.*) injection of HFB provides an optimal approach to tumor oximetry, and should provide measurements comparable to those obtained using electrodes. In addition, this minimally invasive approach facilitates mapping of dynamic changes in pO_2 with respect to interventions.

Methods

Dunning prostate adenocarcinomas (R3327-AT1) were implanted in male Copenhagen rats (~250 g), as described in detail previously [15]. Tumors were divided

into two groups and allowed to grow to about $\sim 2 \text{ cm}^3$ or $> 3.5 \text{ cm}^3$ volume. For MR investigations rats were placed under general gaseous anesthesia with 33% inhaled O_2 ($0.3 \text{ dm}^3/\text{min}$ O_2 , $0.6 \text{ dm}^3/\text{min}$ N_2O , and 0.5% methoxyflurane. Hexafluorobenzene (25 - 40 μl) was injected directly into the tumors in both central and peripheral regions using a Hamilton syringe with a custom made fine sharp needle (32 G). A fiber optic probe was placed rectally to monitor core temperature. NMR experiments were performed using an Omega CSI 4.7 Tesla horizontal bore magnet system with actively shielded gradients with a tunable ($^1\text{H}/^{19}\text{F}$) single turn size-matched solenoid coil placed around the tumor. Following traditional imaging to establish the distribution of HFB, tumor oxygenation was estimated on the basis of ^{19}F PDSR EPI relaxometry of the HFB [10] with a typical 1.25 mm in plane resolution. For initial work three consecutive R1 measurements were made over a period of 1 hour to investigate reproducibility, and stability of the system when the rats breathed 33% O_2 (baseline). Since R1 is a linear function of $p\text{O}_2$ at constant temperature, $p\text{O}_2$ was estimated on a voxel by voxel basis using the relationship $p\text{O}_2 \text{ (torr)} = (\text{R1} - 0.074)/0.0016$ [10]. The inhaled gas was then altered to 100% oxygen, and relaxation measurements (three) were immediately repeated over a period of 1 hour. Finally, the gas was switched back to the baseline state and three further $p\text{O}_2$ determinations were immediately performed over 1 hour. Our initial studies required 20 mins to produce a $p\text{O}_2$ map, but more recent introduction of the ARDVARC acquisition protocol [12] provides enhanced maps in 8 mins. Breast 13762 NF adenocarcinomas were examined similarly.

Histography was applied to groups of size matched tumors, which did not receive HFB. Halothane was used in place of methoxyflurane. Using the Eppendorf Histograph 100 to 200 individual $p\text{O}_2$ determinations were made in each tumor, as recommended by the manufacturer. For dynamic measurements a Diamond General micro-electrode (700 μm) was inserted to a specific location. Baseline $p\text{O}_2$ was measured and the inhaled gas altered to 100% O_2 or carbogen (95% O_2 /5% CO_2) for 30 mins. At this stage $p\text{O}_2$ was

again measured. Following a series of measurements with different gases at one location, the needle was moved and the gases cycled again.

Statistical significance of changes in oxygenation was assessed using analysis of variance (ANOVA) on the basis of Fisher PLSD. Experiments were approved by the Institutional Animal Care and Advisory Committee conducted in accordance with National Laws.

Results

Both FREDOM and electrode methods indicated similar oxygen tension distributions for the AT1 tumors (Fig. 1). Moreover, both techniques showed that tumors with volume $> 3.5 \text{ cm}^3$ were significantly ($p < 0.0001$) less well oxygenated than smaller tumors (volume $< 2 \text{ cm}^3$). For the large tumors FREDOM indicated median $p\text{O}_2 = 2$ torr and fraction < 10 torr (HF_{10}) = 82 %, while the Eppendorf electrode indicated median $p\text{O}_2 = 3$ torr and $\text{HF}_{10} = 84\%$. For the small tumors the match was less good with median = 15 v 8 torr and $\text{HF}_{10} = 44$ versus 66% for FREDOM and electrode, respectively. Examination of the MR images showed that for 1 small tumor most of the HFB resided very close to the tumor edge and may have biased the apparent $p\text{O}_2$. Indeed, if this tumor was excluded there was no significant difference between the respective $p\text{O}_2$ distributions.

Using the FREDOM approach we also examined response to respiratory challenge. Increasing the concentration of inspired oxygen from 33% to 100% O_2 produced a significant increase ($p < 0.0001$) in tumor oxygenation for the group of small tumors. In contrast no change was observed in the mean $p\text{O}_2$ for the group of large tumors. A strength of the FREDOM approach is the ability to follow individual tumor regions, with respect to intervention, in this case respiratory challenge. Six representative regions were selected from a single tumor (Fig. 2a). Three regions, which were initially well oxygenated ($p\text{O}_2 > 10$ torr) showed rapid and significant increases within 8 minutes of switching from 33% O_2 to 100% O_2 . Changes in relatively poorly oxygenated regions

were much slower, although 2 of 3 regions did show a significant change in pO₂ after 24 mins.

Electrode investigation of dynamic changes in pO₂ also showed 3 of six regions with significant changes in switching from 33% O₂ to 100% O₂, but only 1 region was also significantly different with carbogen (Fig. 2b).

In a representative large breast tumor (~ 4 cm³) we found significant changes in pO₂ (p < 0.0001) with respect to respiratory challenge with baseline mean pO₂ = 40±3 rising to mean pO₂ = 99±4, when rat inhaled carbogen and mean pO₂ = 145 ±4 for oxygen inhalation.

Discussion

These results demonstrate the similarity of measurements obtained using traditional electrodes or the new FREDOM approach to tumor oximetry. In each case there was a significant difference in pO₂ observed in small versus large AT1 tumors. For larger tumors the hypoxic fraction, mean and median were very similar, together with the range of typical pO₂ values. In smaller tumors MR suggested a larger range with a number of measurements in excess of 100 torr. This may have arisen from measurements close to the tumor periphery, which are less common using electrodes.

A significant strength of the FREDOM approach is the ability to monitor dynamic changes in regional pO₂ in response to acute interventions. Others have used the Eppendorf system to examine acute changes [16], but this required reintroduction of the needle electrode and generation of new tracks. Not only was this invasive, but it also led to sampling of parallel tissue regions rather than the fate of specific regions. Given the extensive heterogeneity encountered in tumors and steep local gradients in pO₂ we believe it will be valuable to follow individual tumor regions. Historically, regional response to intervention was assessed by placing an electrode at a specific location and monitoring changes in pO₂ [17]. We have now performed such experiments with a micro

electrode and found a range of baseline pO_2 values and response to respiratory challenge similar to those seen using MRI.

We have now shown both that there is distinct intra tumoral heterogeneity in baseline oxygenation in the Dunning prostate AT1 tumor and also in the response to intervention. In common with our previous observations a three fold change in FO_2 seems to lead to a threefold response in tumor pO_2 . However, the rate of change is highly variable. Preliminary data with 8 min time resolution suggest that well oxygenated regions respond rapidly, whereas those poorly oxygenated require much longer. Such observations could have significant implications for patient inhalation times prior to therapy: while previous work had shown that Pre Irradiation Breathing Times (PIBT) could substantially influence the effect of oxygen or carbogen breathing [18], the differential response of individual tumor regions may not have been fully appreciated.

In developing a new technique it is important to demonstrate its reliability, robustness and general application. We and several other groups have now applied the FREDOM approach to tumor oximetry. Initially investigators favored intra venous or intra peritoneal administration of emulsions of fluorocarbons. While material became trapped in tumors and could be used to report pO_2 [19-22], it became increasingly apparent that material delivered via the vasculature tended to bias measurements towards well perfused tumor regions [22]. Indeed, recent measurements by Griffiths *et al.* have confirmed such a bias [23]. Furthermore, the use of emulsions to carry the PFCs tend to lead to extensive uptake by the reticuloendothelial system with hepatomegaly. Intra tumoral administration is minimally invasive provided that a fine sharp needle is applied, as we have used here. We have now extended our work from the Dunning prostate R3327-AT1 tumor, which is poorly differentiated, has only microscopic necrotic foci and is firm, to the 13762 breast tumor, which has less structure and considerable cystic fluid. Here, we have simply reported the ability to measure dynamic changes in the breast tumor oxygenation, but in the accompanying work (Song *et al.*, this volume), we show more extensive results.

Since the MR and electrode approaches appear to give similar results one may debate the relative their merits. Clearly, MR is very expensive, with a typical imaging system costing upwards of \$1 M, compared with \$60 000 for the Eppendorf and < \$5 000 for a laboratory micro electrode system. However, MR facilitates the simultaneous measurements of dynamic changes in response to intervention at multiple points within a tumor. While we were able to follow changes in pO₂ at specific regions using a needle electrode with placement at sequential locations accompanied by cycling of the intervention, such an approach would be less satisfactory for other interventions, and even here, may have led to some conditioning or hysteresis. The FREDOM approach may be readily combined with other measurements such as blood flow/perfusion [24], pH [25] or metal ions by infusion of appropriate reporter molecules [26].

As a reporter molecule HFB has many advantageous properties. It is cheap, readily available, and exhibits minimal acute toxicity (LD₅₀ > 25 g/kg) [27]. No signs of renal or hepatic toxicity have been found [28] and others have tested doses as high as 50 g/kg (twice weekly) orally in rats over 35 weeks [29]. We typically find substantial clearance from tumors within 24 h, though this does limit our measurements to acute response to interventions [12]. High symmetry within the molecule leads to a single ¹⁹F MR resonance providing optimal SNR. The R1 (=1/T1) is highly sensitive to pO₂ while showing little response to temperature [9]. Long T1s up to 14 s appear to make HFB less efficient for spin lattice relaxometry, but use of the pulse burst saturation recovery approach minimizes the length of th experiment [10] and a large range of T1 values is a requisite for sensitivity to changes in pO₂. The long transverse relaxation time (T2) is ideally suited to echo planar imaging.

The ultimate value of a novel technique will depend on its adoption by multiple laboratories, and the significance of the results that can be generated. We believe that the FREDOM approach is versatile and we are demonstrating increasing applications, and thus, we foresee expanded future application of the technique.

Reference:

1. Hall EJ. The oxygen effect and reoxygenation. In: Hall EJ, ed. *Radiobiology for the Radiologist*. 3 ed. Philadelphia: Lippincott, J. B., 1994: 133-152.
2. Chapman JD, Stobbe CC, Arnfield MR, Santus R, Lee J, McPhee MS. Oxygen Dependency of Tumor Cell Killing *In Vitro* by Light Activated Photofrin II. *Radiat. Res.* 1991;126:73-79.
3. Brown JM, Giaccia AJ. Tumor hypoxia: the picture has changed in the 1990s. *Int. J. Radiat. Biol.* 1994;65:95-102.
4. Vaupel PW, Höckel M. Oxygenation status of human tumors: a reappraisal using computerized pO₂ histography. In: Vaupel PW, Kelleher DK, Günderoth M, eds. *Tumor Oxygenation*. Stuttgart: Gustav Fischer, 1995: 219-232. (Thews G, ed. *Funktionsanalyse biologischer Systeme*; vol 24).
5. Fyles AW, Milosevic M, Wong R, et al. Oxygenation predicts radiation response and survival in patients with cervix cancer. *Radiother. Oncol.* 1998;48:149-56.
6. Höckel M, Schlenger K, Aral B, Mitze M, Schäffer U, Vaupel P. Association between tumor hypoxia and malignant progression in advanced cancer of the uterine cervix. *Cancer Res.* 1996;56:4509-15.
7. Nordmark M, Overgaard M, Overgaard J. Pretreatment oxygenation predicts radiation response in advanced squamous cell carcinoma of the head and neck. *Radiother. Oncol.* 1996;41:31-40.
8. Stone HB, Brown JM, Phillips T, Sutherland RM. Oxygen in human tumors: correlations between methods of measurement and response to therapy. *Radiat. Res.* 1993;136:422-434.
9. Mason RP, Rodbumrung W, Antich PP. Hexafluorobenzene: a sensitive ¹⁹F NMR indicator of tumor oxygenation. *NMR in Biomed.* 1996;9:125-134.

10. Le D, Mason RP, Hunjan S, Constantinescu A, Barker BR, Antich PP. Regional tumor oxygen dynamics: ^{19}F PBSR EPI of hexafluorobenzene. *Magn. Reson. Imaging*, 1997;15(8):971-81.
11. Mason RP, Constantinescu A, Hunjan S, et al. Regional tumor oxygenation and measurement of dynamic changes. *Radiat. Res.* 1999;152:239.
12. Hunjan S, Mason RP, Constantinescu A, Peschke P, Hahn EW, Antich PP. Regional tumor oximetry: ^{19}F NMR spectroscopy of hexafluorobenzene. *Int. J. Radiat. Oncol. Biol. Phys.* 1998;40(5):161-71.
13. Delpuech J-J, Hamza MA, Serratice G, Stébé M-J. Fluorocarbons as oxygen carriers. I. An NMR study of oxygen solutions in hexafluorobenzene. *J. Chem. Phys.* 1979;13:399.
14. Mason RP. Non-invasive physiology: ^{19}F NMR of perfluorocarbon. *Art. Cells, Blood Sub. & Immob. Biotech.* 1994;22(4):1141-1153.
15. Hahn EW, Peschke P, Mason RP, Babcock EE, Antich PP. Isolated tumor growth in a surgically formed skin pedicle in the rat: a new tumor model for NMR studies. *Magn. Reson. Imaging* 1993;11:1007-1017.
16. Laurence V, Ward R, Bleehen N. Tumor pO_2 distribution in patients treated with the combination of nicotinamide and carbogen breathing. In: P. W. Vaupel, D. K. Kelleher, M. Günderoth, eds. *Tumor Oxygenation*. Stuttgart: Gustav Fischer., 1995: 185-193.
17. Cater D, Silver I. Quantitative measurements of oxygen tension in normal tissues and in the tumors of patients before and after radiotherapy. *Acta Radiol.* 1960;53:233-256.
18. Chaplin DJ, Horsman MR, Siemann DW. Further evaluation of nicotinamide and carbogen as a strategy to reoxygenate hypoxic cells *in vivo*: importance of nicotinamide dose and pre-irradiation breathing time. *Br. J. Cancer* 1993;68:269-73.

19. Dardzinski BJ, Sotak CH. Rapid tissue oxygen tension mapping using ^{19}F Inversion-recovery Echo-planar imaging of Perfluoro-15-crown-5-ether. *Magn. Reson. Med.* 1994;32(1):88-97.
20. Baldwin NJ, Ng TC. Oxygenation and metabolic status of KHT tumors as measured simultaneously by ^{19}F magnetic resonance imaging and ^{31}P magnetic resonance spectroscopy. *Magn. Reson. Imaging* 1996;14(5):514-551.
21. Fishman JE, Joseph PM, Carvlin MJ, Saadi-Elmandjra M, Mukherji B, Sloviter HS. *In vivo* measurements of vascular oxygen tension in tumors using MRI of a fluorinated blood substitute. *Invest. Radiol.* 1989;24:65-71.
22. Mason RP, Antich PP, Babcock EE, Constantinescu A, Peschke P, Hahn EW. Non-invasive determination of tumor oxygen tension and local variation with growth. *Int. J. Radiat. Oncol. Biol. Phys.* 1994;29: 95-103.
23. McIntyre DJO, McCoy CL, Griffiths JR. Tumour oxygenation measurements by ^{19}F MRI of perfluorocarbons. *Curr. Sci.* 1999;76:753-762.
24. Brown SL, Ewing JR, Loloosvary A, Butt S, Cao Y, Kim JH. Magnetic Resonance Imaging of perfusion in rat cerebral 9L tumor after nicotinamide administration. *Int. J. Radiat. Oncol. Biol. Phys.* 1999;43:627-33.
25. Mason R, Hunjan S, He S, et al. Tumor trans membrane pH gradient and regional oxygen tension measured by fluorine magnetic resonance. In: Moraes M, Brentani R, Bevilacqua R, eds. 17th International Cancer Congress. Rio de Janeiro: Monduzzi, 1998: 1627-31. vol 2).
26. Mason RP. Transmembrane pH gradients *in vivo*: measurements using fluorinated vitamin B6 derivatives. *Curr. Med. Chem.* 1999;6:533-51.
27. Lancaster. Material Safety Data Sheet. In: Lancaster Synthesis Inc., 1998:
28. Hall LW, Jackson SRK, Massey GM. Hexafluorobenzene in veterinary anaesthesia. In: Arias A, Llaurodo R, Nalda MA, Lunn JN, eds. *Recent Progress in Anaesthesiology and Resuscitation.* Oxford: Excerpta Medica, 1975: 201-204.

29. Rietjens IMCM, Steensma A, den Besten C, et al. Comparative biotransformation of hexachlorobenzene and hexafluorobenzene in relation to the induction of porphyria. *Eur. J. Pharmacol.* 1995;293:292-299.

Figure legends

Figure 1

Comparison of oxygenation in size-matched groups of AT1 tumors based on ^{19}F MR EPI relaxometry (left) and electrode polarography (right), when rats inhaled 33% O_2 . Small tumors are shown at top (volume $< 2 \text{ cm}^3$) and large tumors below (volume $> 3.5 \text{ cm}^3$). Each method shows a significant difference in tumor oxygenation for small versus large tumors ($p < 0.0001$).

Figure 2

a) Dynamic changes in pO_2 of six specific regions of an AT1 tumor. The three high pO_2 regions had significantly different pO_2 (* $p < 0.05$) from those with low pO_2 at each time point. Within 8 mins of elevating inspired O_2 the three high pO_2 voxels had significantly increased pO_2 ($p < 0.05$) while the low pO_2 voxels required > 24 mins to show significant changes. All six regions were observed simultaneously using the FREDOM approach.

b) Dynamic changes in pO_2 of six specific regions of an AT1 tumor. The electrode was placed in one location at a time and inhaled gases cycled for subsequent locations.

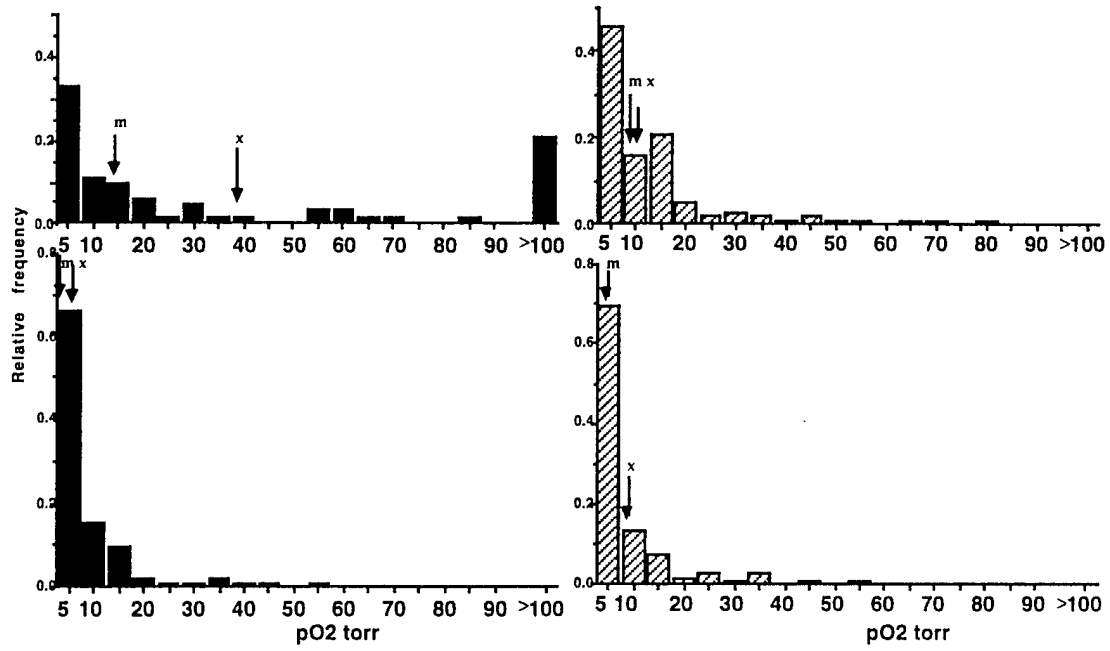


Figure 1

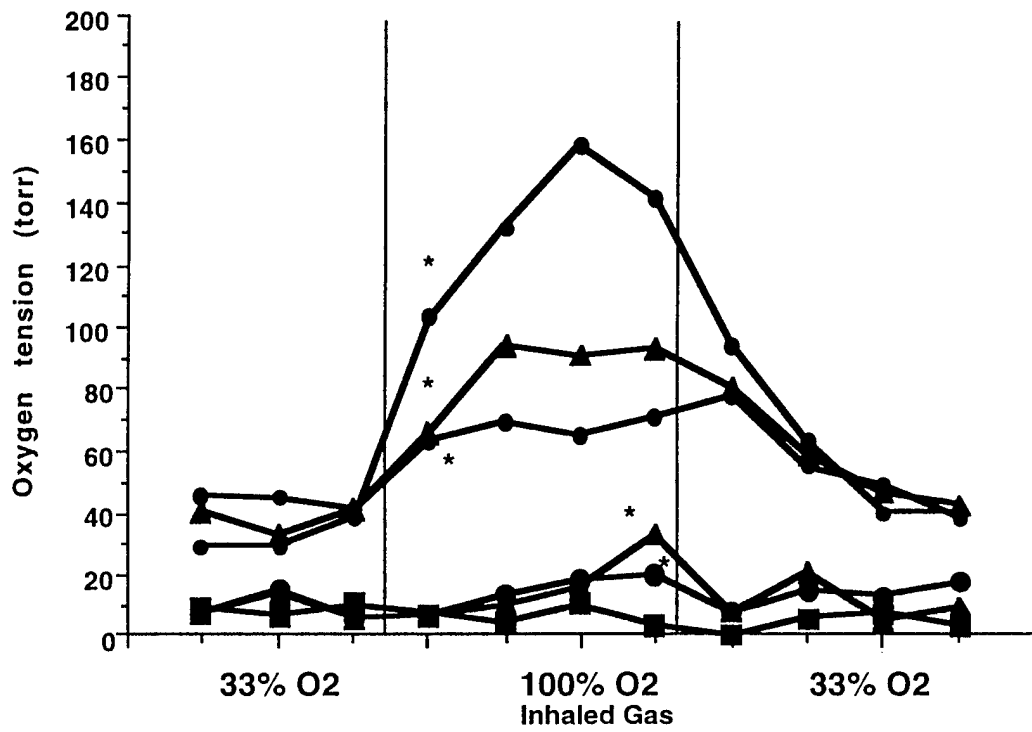


Figure 2a

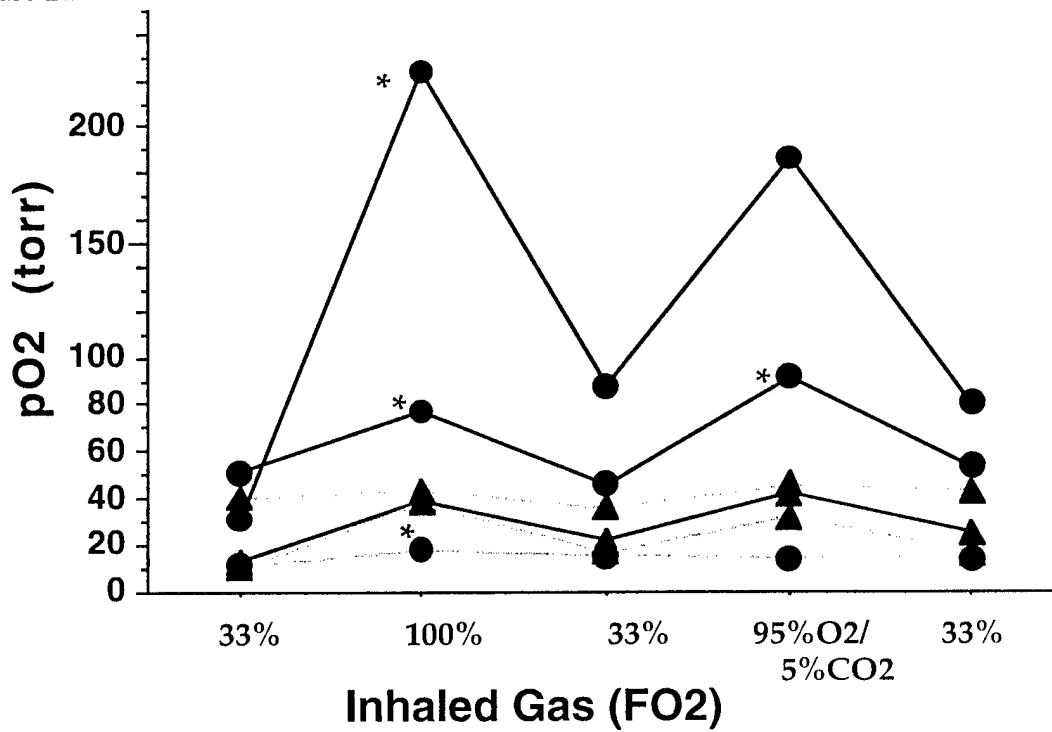


Figure 2b

Regional Tumor Oxygen Tension and Blood Flow: Correlation Studies Using ^{19}F PBSR-EPI of Hexafluorobenzene

Y. Song, R. P. Mason, S. Hunjan, A. Constantinescu, E. W. Hahn, and P. P. Antich,
Department of Radiology, UT Southwestern Medical Center, Dallas, Texas, USA

Introduction: It is recognized that therapeutic efficacy may be influenced by tumor oxygenation. In particular, hypoxic tumors resist radiotherapy. We have recently shown the feasibility of monitoring tumor oxygen tension based on ^{19}F PBSR-EPI of hexafluorobenzene (HFB) [1]. We also found that HFB clears from tumors over a period of hours [2]. Since HFB is a non-ionic freely diffusible tracer, it appeared that clearance rate would provide an indication of relative tumor blood flow (TBF). We have now investigated the feasibility of mapping the clearance rate of HFB and correlating this putative blood flow marker with corresponding $p\text{O}_2$.

Methods: Dunning prostate R3327-AT1 or breast 13762 NF adenocarcinoma was implanted in a skin pedicle on the foreback of a rat. When the tumor reached 1~2 cm diameter, 40 μl HFB were injected directly into the tumor (IT), both centrally and peripherally. The rat was maintained under general gaseous anesthesia (33% O_2 , 66% N_2O and 0.5% methoxyflurane). A homebuilt tunable 2 cm $^1\text{H}/^{19}\text{F}$ single turn solenoid coil was placed around the tumor and MR experiments were performed using a 4.7 T magnet equipped with actively shielded gradients. 3D ^1H images were acquired for anatomical reference and corresponding ^{19}F images were obtained to show the distribution of HFB. Tumor oxygenation was assessed using ^{19}F PBSR-EPI of HFB. By applying the acquisition protocol ARDVARC (Alternated Relaxation Delays with Variable Acquisitions to Reduce Clearance effects) [2], we achieved $R1$ maps in 8 min. A series of maps were acquired over a period of 2 hours with respect to respiratory challenges. $p\text{O}_2$ maps were then generated by applying the relationship: $p\text{O}_2(\text{torr}) = [R1(s^{-1}) - 0.074]/0.0016$ to the $R1$ maps. The data also allowed us to produce a clearance map based on EPI images with the longest delay (90 s).

Results: $p\text{O}_2$ maps were generated with a typical precision of 2 ~ 5 torr and 30 ~ 100 individual voxels within a tumor. For many regions, the HFB signal intensity was found to decline exponentially with a typical clearance half-life ranging from $T_{1/2} = 700$ to 1200 min, though many voxels indicated no apparent changes.

Discussion: Regional tumor oxygen tension and blood flow are important physiological parameters and the opportunity to measure both simultaneously would be of value in physiological research. Based on the preliminary data presented here, we believe that clearance of HFB provides an indication of relative TBF by analogy with studies of cerebral blood flow using freon-23 [3]. In future studies, such measurements will be rigorously evaluated.

References:

- [1] D. Le, *et al.*, *MRI*, **15**, 971-981 (1997). [2] S. Hunjan, *et al.*, *IJROBP*, **41**, 161-171 (1998)
[3] J. R. Ewing, *et al.*, *Stroke*, **21**, 100-106 (1990).

This study was supported in part by grants from The American Cancer Society (RPM), The Whitaker Foundation (RPM), the DOD Breast Cancer Initiative (YS), and NIH BRTP.

TUMOR OXYGEN DYNAMICS: COMPARISON BETWEEN ^{19}F MR-EPI OF HEXAFLUOROBENZENE AND FREQUENCY DOMAIN NIR SPECTROSCOPY

Song^{1,2}, Y.; Worden¹, K. L.; Jiang¹, X.; Zhao², D.; Constantinescu², A.; Liu¹, H.; and Mason², R. P.

¹Joint Graduate Program in Biomedical Engineering,

²Department of Radiology, UT Southwestern Medical Center, Dallas, TX 75235, USA

Introduction: Oxygen plays a key role in tumor therapy and may be related to tumor development: e.g., angiogenesis and metastasis. Using noninvasive techniques to accurately measure oxygenation could assist in developing novel therapies. Here, we have used ^{19}F MR-EPI relaxometry of hexafluorobenzene (HFB)[1] to monitor tissue oxygen tension ($p\text{O}_2$) of rat breast tumors and compared the results with changes in hemoglobin saturation ($s\text{O}_2$) and concentration in the vasculature of the tumors observed using a new dual wavelength homodyne near-infrared (NIR) system.

Methods: Breast 13762 NF adenocarcinomas were implanted in skin pedicles on the forebacks of adult female Fischer rats. Once the tumors reached $\sim 1\text{cm}$ diameter, the tumor blood $s\text{O}_2$ was assessed by NIR spectroscopy using a dual wavelength NIR system (758 nm and 782 nm) in transmission geometry [2]. The tumor blood volume and $s\text{O}_2$ were calculated from the light amplitude. The rats were maintained under general gaseous anesthesia (33% O_2 , 66% N_2O and 0.5% methoxyflurane). Once stable baseline measurements were achieved, the inhaled gas was altered to pure oxygen or carbogen and dynamic changes were observed over a period of two hours. Both the magnitude and rate of change of $s\text{O}_2$ were examined. Following the NIR experiments, 40 μl HFB were injected directly into both central and peripheral regions of the tumors. A tunable 2 cm $^1\text{H}/^{19}\text{F}$ single turn solenoid coil was placed around the tumor and MR experiments were performed using a 4.7 T magnet. Regional tumor $p\text{O}_2$ was estimated using the relationship: $p\text{O}_2$ (torr) = $[R1 - 0.074]/0.0016$, where $R1$ is the spin lattice relaxation rate of HFB. Twenty-three $p\text{O}_2$ maps were produced in 3 hours with respect to respiratory challenge.

Results: NIR showed significant changes in vascular oxygenation accompanying respiratory interventions. ^{19}F MR-EPI also showed significant changes in tissue $p\text{O}_2$, with considerable regional heterogeneity in both absolute values and rate of change accompanying interventions. Generally, changes in vascular $s\text{O}_2$ preceded tissue $p\text{O}_2$, particularly for smaller tumors.

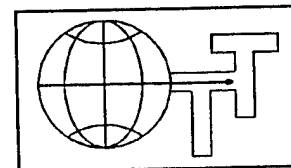
Discussion: Regional tumor $p\text{O}_2$ and blood $s\text{O}_2$ are important physiological parameters. The capability to measure them will provide insight into progressive physiological changes in a tumor accompanying interventions. NIR has the advantage of being entirely noninvasive, but the MRI approach clearly reveals detailed oxygenation heterogeneity. We believe that better understanding and monitoring of tumor oxygenation can lead to improved tumor therapy.

References:

[1] D. Le, *et al.*, *MRI*, **15**, 971-981 (1997). [2] K. Worden, *et al.*, *SPIE*, **3597** (1999)

Acknowledgments:

Supported in part by grants from The American Cancer Society (RPM), The Whitaker Foundation (RPM and HL), the DOD Breast Cancer Initiative (YS), and NIH BRTP.



Molecular Determinants of Sensitivity to Anti tumor Agents

Tumor oxygenation and measurement of regional dynamic changes

Ralph P. Mason, Sandeep Hunjan, Anca Constantinescu, Yulin Song, Eric W. Hahn, and Peter P. Antich, Advanced Radiological Sciences, U.T. Southwestern Medical Center, Dallas, Texas and Christian Blum and Peter Peschke, Deutsches Krebsforschungszentrum, Heidelberg, Germany

Therapeutic efficacy may be influenced by tumor oxygenation. In particular, hypoxic tumors resist radiotherapy and may be good candidates for hypoxia selective cytotoxic agents. We recently described a novel approach to measuring regional tumor oxygen tension using ^{19}F pulse burst saturation recovery (PBSR) nuclear magnetic resonance (NMR) echo planar imaging (EPI) relaxometry of hexafluorobenzene (HFB) (1). We have now compared oxygen tension measurements in a group of size matched Dunning prostate rat tumors R3327-AT1 made using this new method with a traditional polarographic method: the Eppendorf Histograph. We also demonstrate extension of the MR techniques to rat breast tumors.

Methods: Rat Dunning prostate R3327-AT1 or breast 13762 NF adenocarcinomas were examined at a volume $< 2 \text{ cm}^3$ or $> 3.5 \text{ cm}^3$: for MRI 40 μl HFB were injected directly into the tumor, both centrally and peripherally. The rat was maintained under general gaseous anesthesia (33% O_2 , 66% N_2O and 0.5% methoxyflurane). A tunable 2 cm $^1\text{H}/^{19}\text{F}$ single turn solenoid coil was placed around the tumor and MR experiments were performed using a 4.7 T magnet equipped with actively shielded gradients. Tumor oxygenation was assessed using ^{19}F PBSR-EPI of HFB. By applying the acquisition protocol ARDYARC (Alternated Relaxation Delays with Variable Acquisitions to Reduce Clearance effects), we achieved R1 maps in 8 min. A series of maps was acquired over a period of 2 hours with respect to respiratory challenges. pO_2 maps were then generated by applying the relationship: $\text{pO}_2 \text{ (torr)} = (\text{R1} - 0.074)/0.0016$. In parallel experiments pO_2 was determined polarographically.

Results: Similar oxygen tension distributions were found using ^{19}F MRI or polarography and both techniques showed that tumors with volume $> 3.5 \text{ cm}^3$ were significantly ($p < 0.0001$) less well oxygenated than smaller tumors (volume $< 2 \text{ cm}^3$). Using the ^{19}F EPI approach we also examined response to respiratory challenge. Increasing the concentration of inspired oxygen from 33% to 100% O_2 produced a significant increase ($p < 0.0001$) in tumor oxygenation for a group of small tumors. In contrast no change was observed in the mean pO_2 for a group of large tumors. Consideration of individual tumor regions, irrespective of tumor size showed a strong correlation between the maximum pO_2 observed when breathing 100% O_2 , as compared with mean baseline pO_2 .

Conclusions: These results further demonstrate the usefulness of ^{19}F EPI to assess changes in regional tumor oxygenation. The ability to measure pO_2 could be valuable in pre-clinical evaluation of novel therapies and ultimately allow therapy to be individualized and optimized for patients.

This work was supported in part by The American Cancer Society (RPM), The Whitaker Foundation (RPM), DOD Breast Cancer Initiative (YS), Verein zur Förderung der Krebserkennung und Krebsbehandlung e.V. Heidelberg (PP) and the NIH BRTP Facility #5-P41-RR02584.

1. D. Le, R. P. Mason, S. Hunjan, A. Constantinescu, B. R. Barker and P. P. Antich, Regional tumor oxygen dynamics: ^{19}F PBSR EPI of hexafluorobenzene. *Magn. Reson. Imaging*, 15, 8, 971-81 (1997).